



Homeland Security

Science and Technology

System Design Considerations for CAXSI: *Coded Aperture X-ray Scatter Imaging*

Joseph A. (Jody) O'Sullivan
and the CAXSI Team



DHS S&T: HSHQDC-11-C-00083

DISP



Massachusetts
Institute of
Technology



THE UNIVERSITY
of NORTH CAROLINA
at CHAPEL HILL

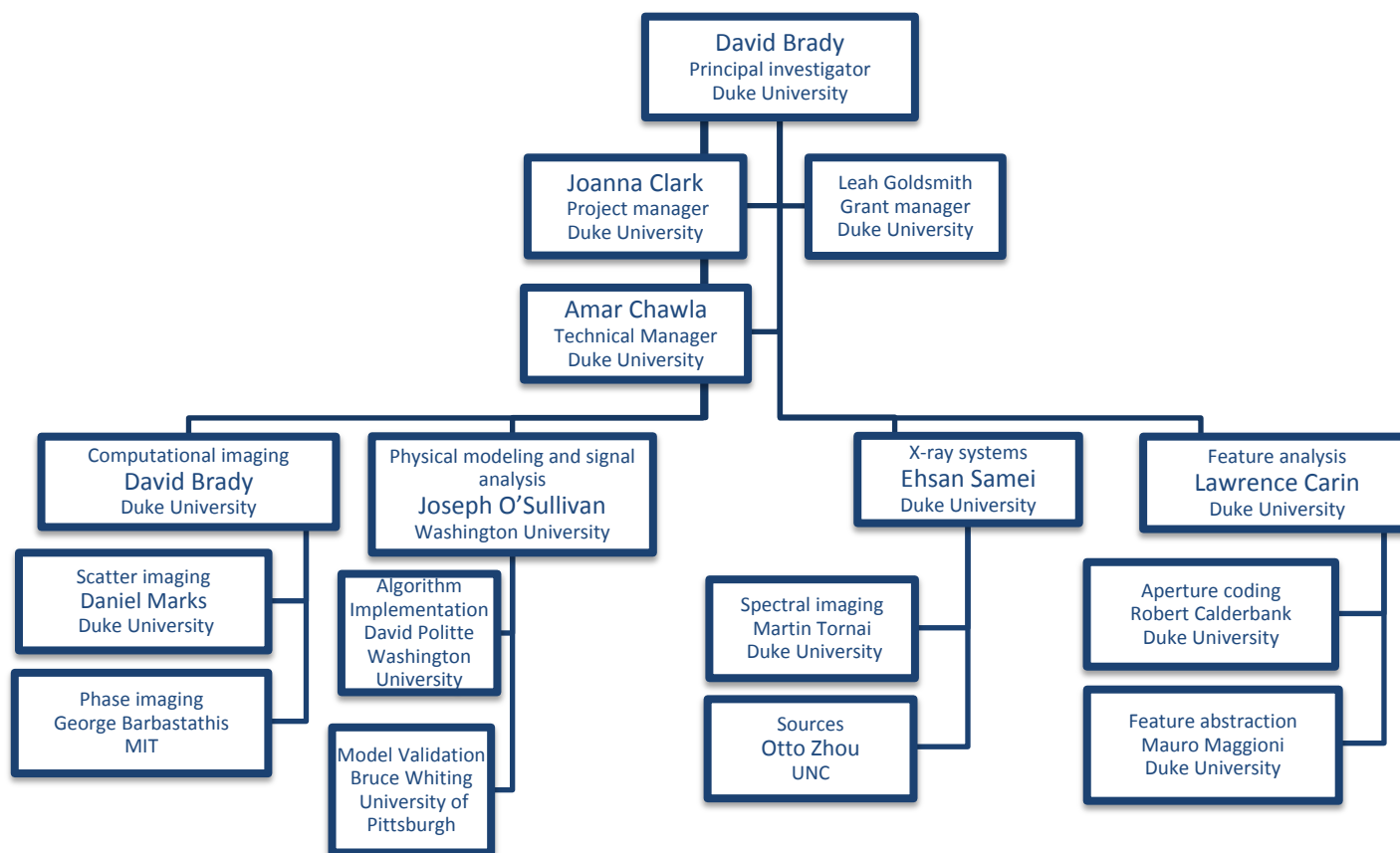


CAXSI Team

- David Brady, Larry Carin, Robert Calderbank, Amarpreet Chawla, Anuj Kapadia, Kalyani Krishnamurthy, Andrew Holmgren, Pooyan Bagherzadeh, Ehsan Samei, Martin Tornai, Mauro Maggioni, Randy McKinley, Scott Wolter, Duke University
- Jody O'Sullivan, David Politte, Ikenna Odinaka, Washington University
- Bruce Whiting, University of Pittsburgh
- Otto Zhou, Kenneth MacCabe, UNC
- George Barbastathis, Jon Petrocelli, Lei Tian, MIT

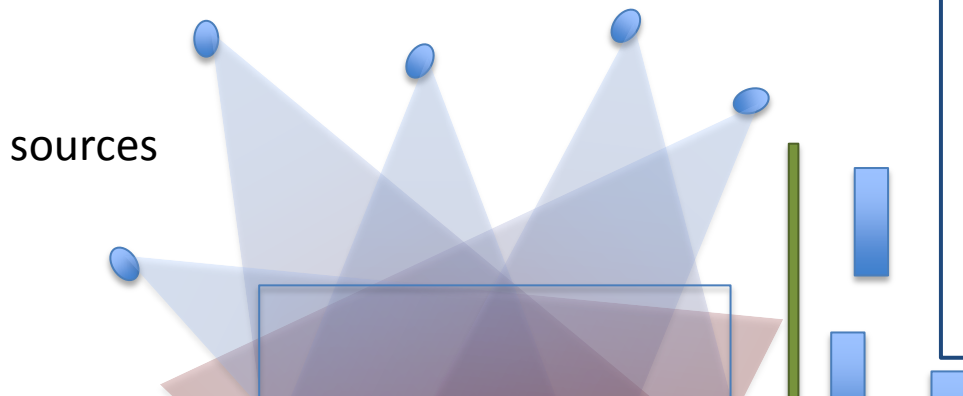


CAXSI Team



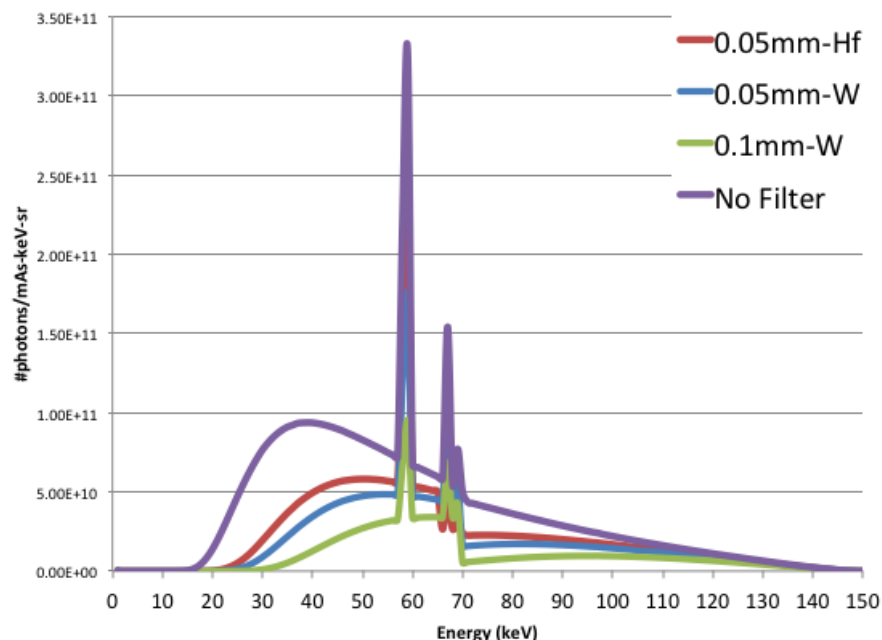
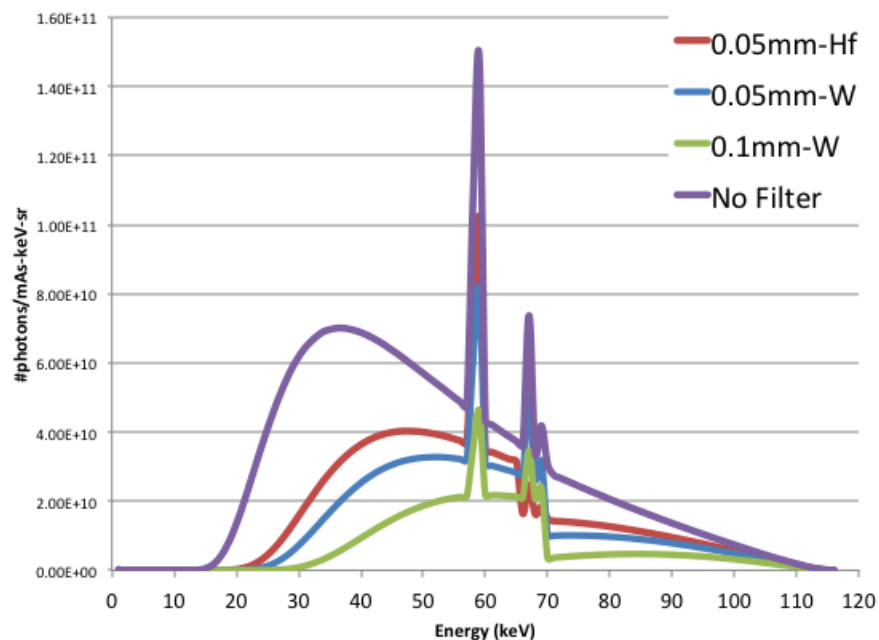


CAXSI System Vision



Selected Key Components

- Distributed sources
 - Novel sources
 - Spectra
 - Primary aperture
- Various detectors
- Coded aperture(s)





CAXSI System Vision

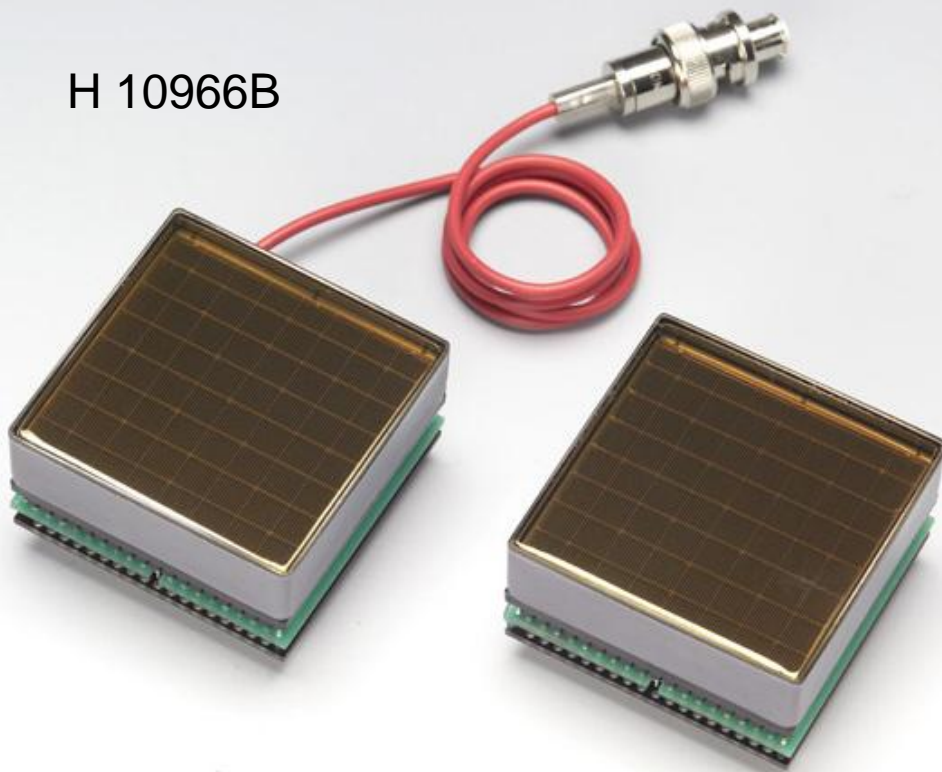
Selected Key Components

- Distributed sources
 - Novel sources
 - Spectra
 - Primary aperture

Various detectors
Coded aperture(s)

sources

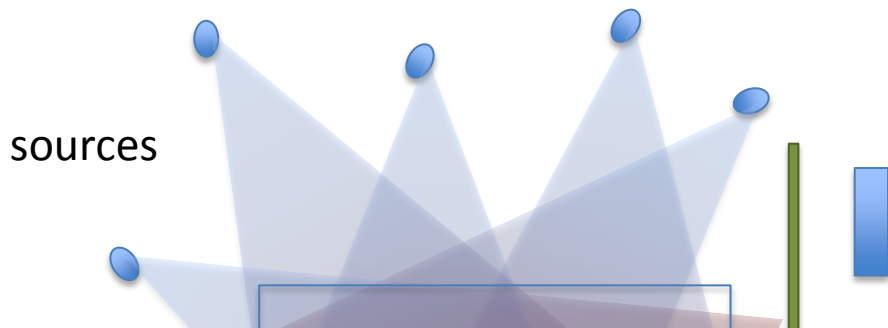
H 10966B



ectors

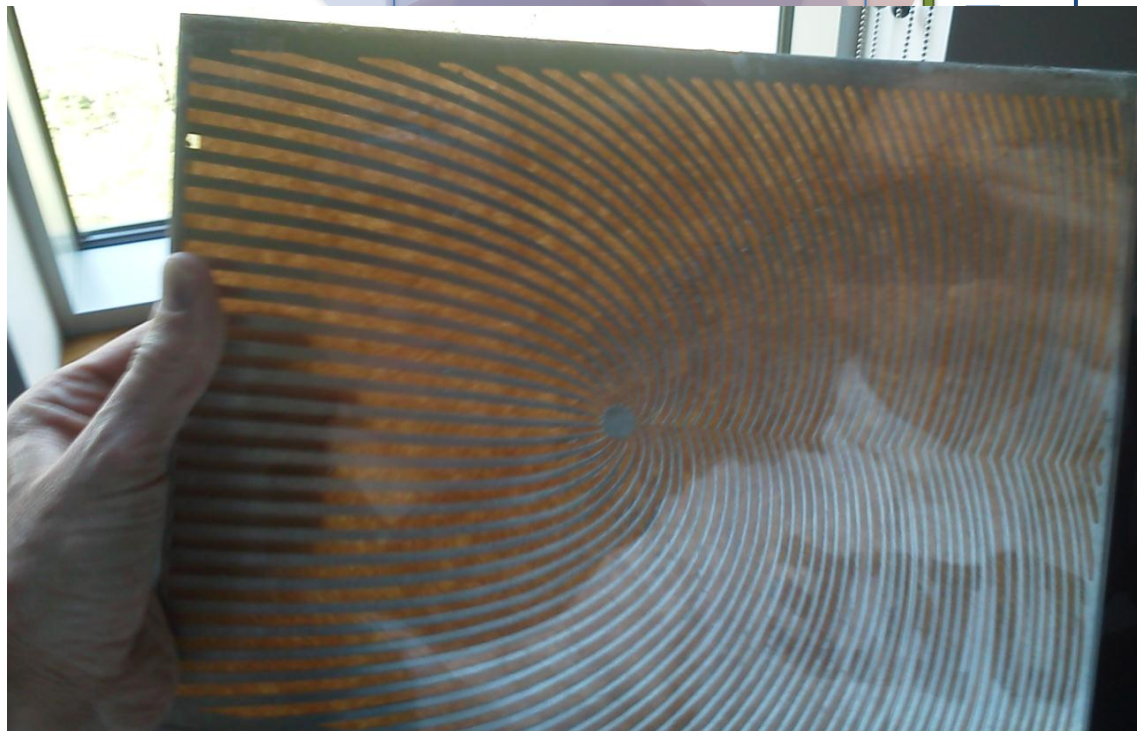


CAXSI System Vision



Selected Key Components

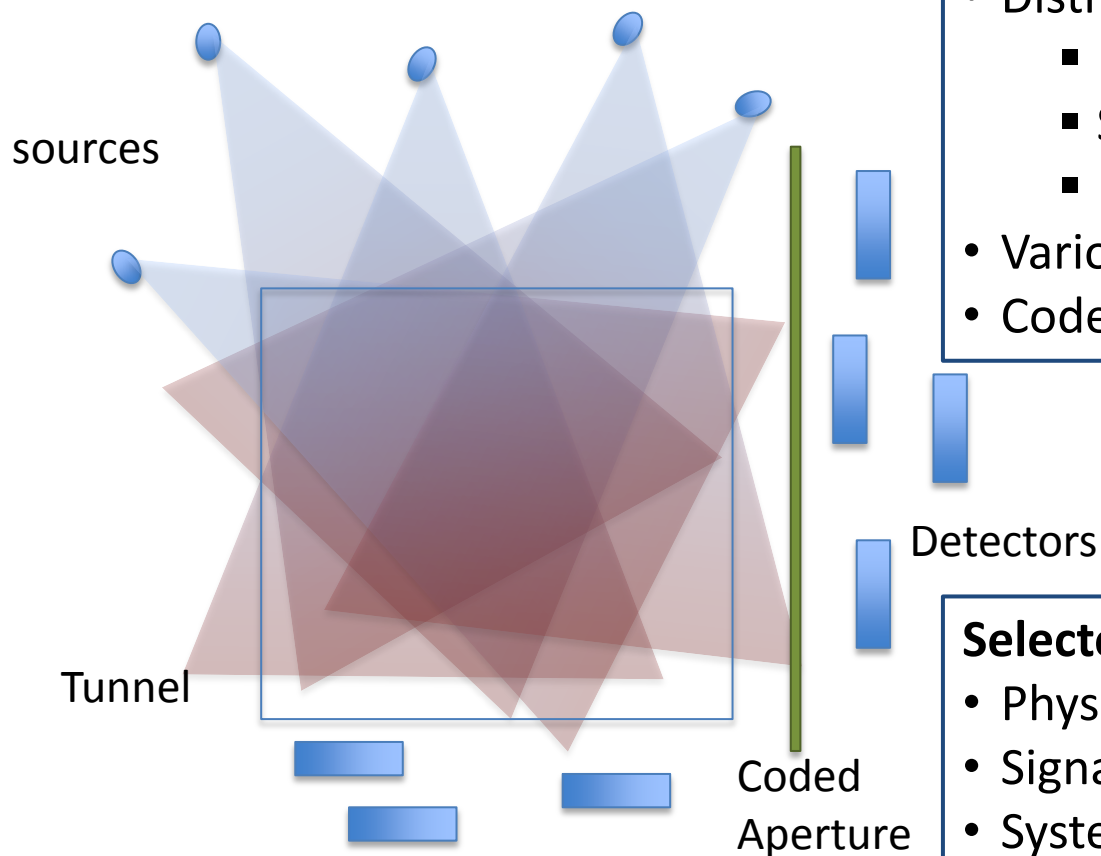
- Distributed sources
 - Novel sources
 - Spectra
 - Primary aperture
- Various detectors
- Coded aperture(s)



ctors



CAXSI System Vision



Selected Key Components

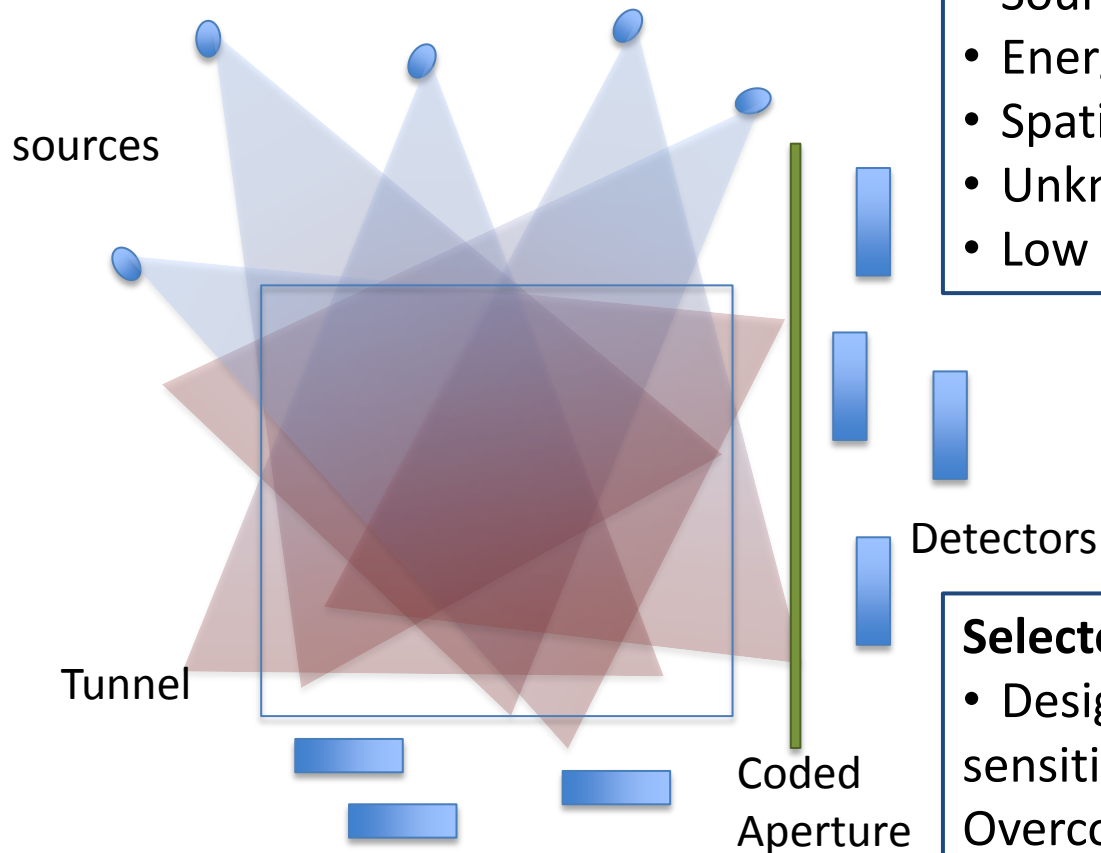
- Distributed sources
 - Novel sources
 - Spectra
 - Primary aperture
- Various detectors
- Coded aperture(s)

Selected Key Ideas

- Physical modeling of signals
- Signature characterization
- System design motivated by integrated sensing and processing (compressive sensing)
- Integration of components



CAXSI System Vision



Selected Key Limitations

- Source spectral width
- Energy sensitivity of detectors
- Spatial extent of targets
- Unknown clutter in the luggage
- Low signal

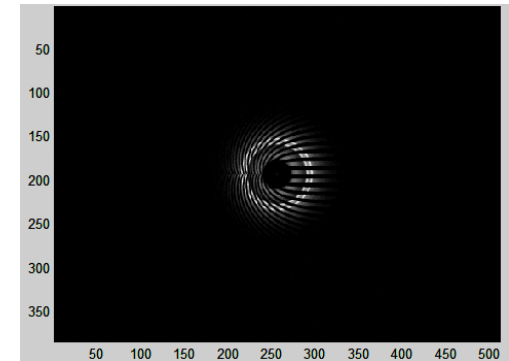
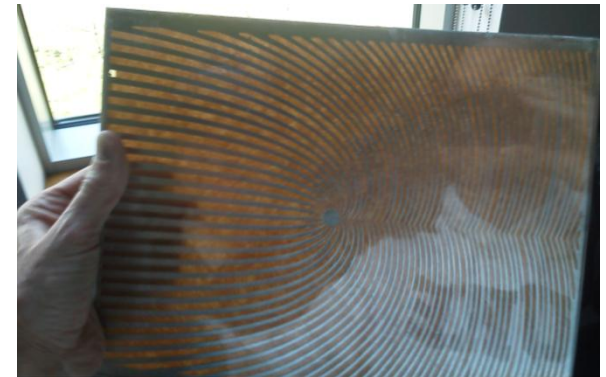
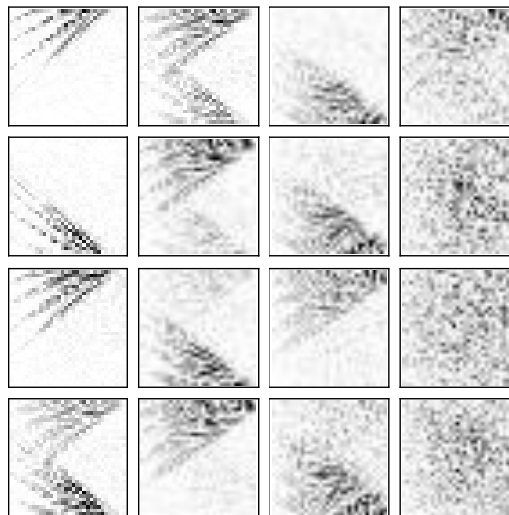
Selected Key Ideas

- Design system to increase sensitivity and specificity → Overcome blurring effects, optimally measure photons
- Multifaceted design space

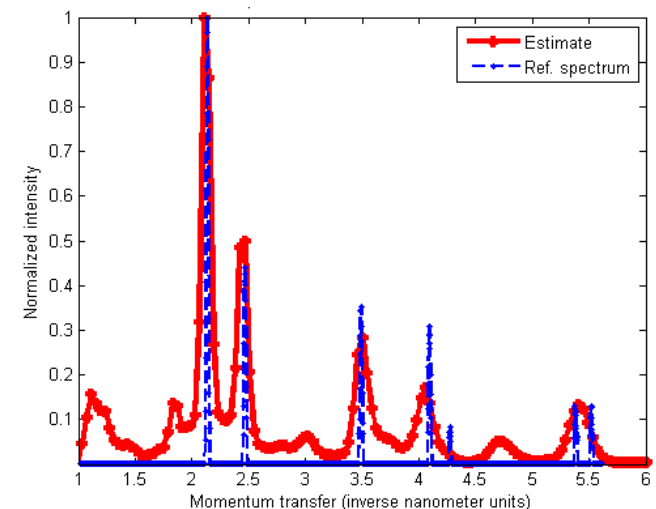


CAXSI Outline

- CAXSI System Vision
- Signature Analysis
 - Measurement space signature
Forward models
 - Object space signature
Reconstruction
 - Logical space signature
SVD
- Conclusion

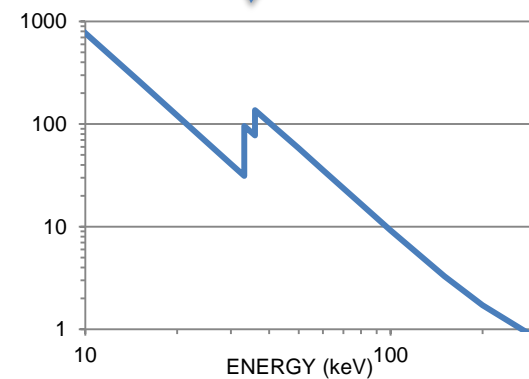
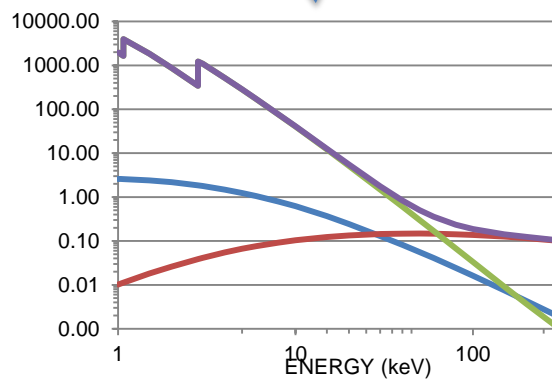
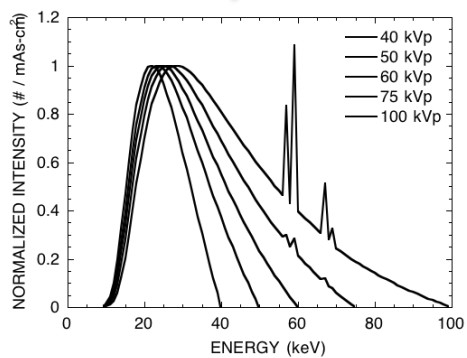
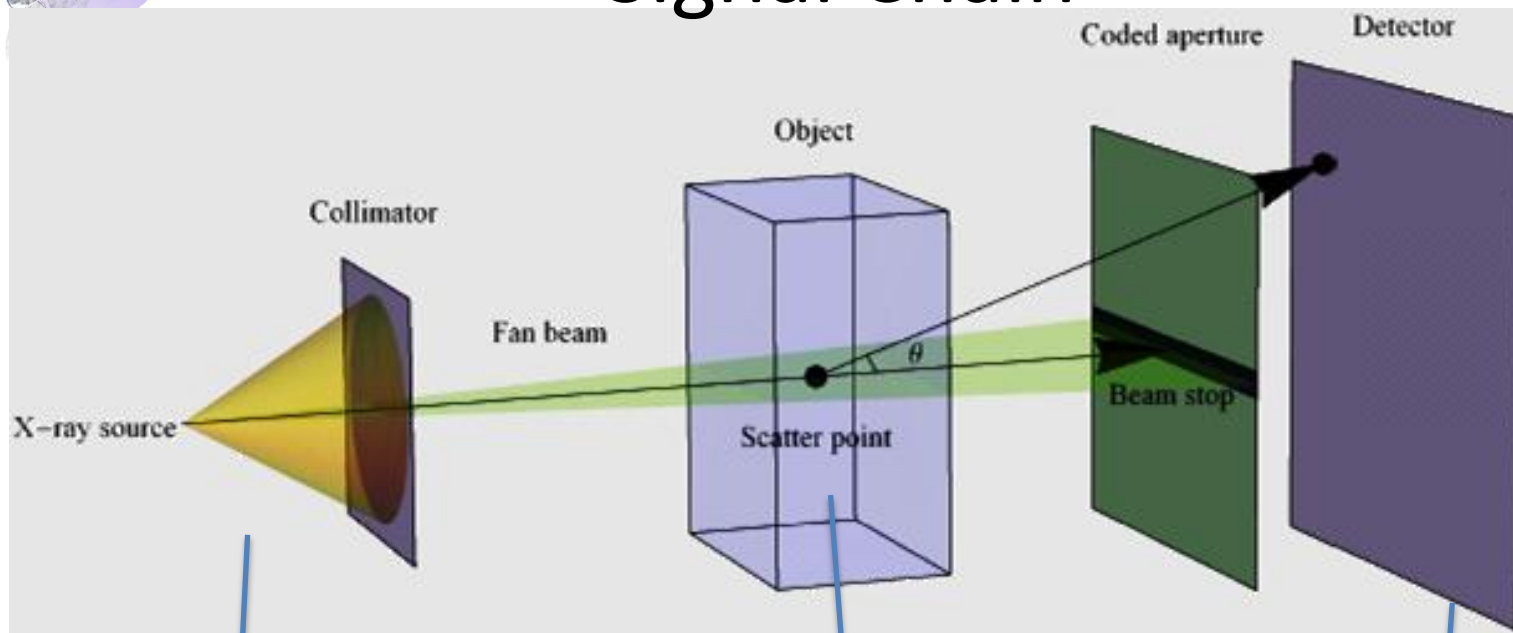


AI





Signal Chain



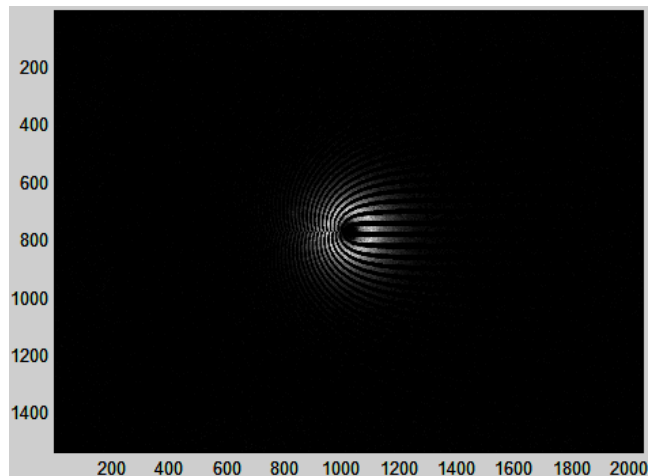
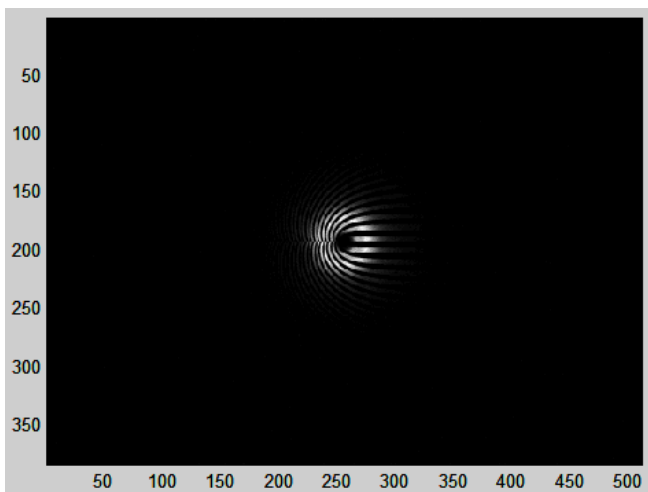


Signature Definition

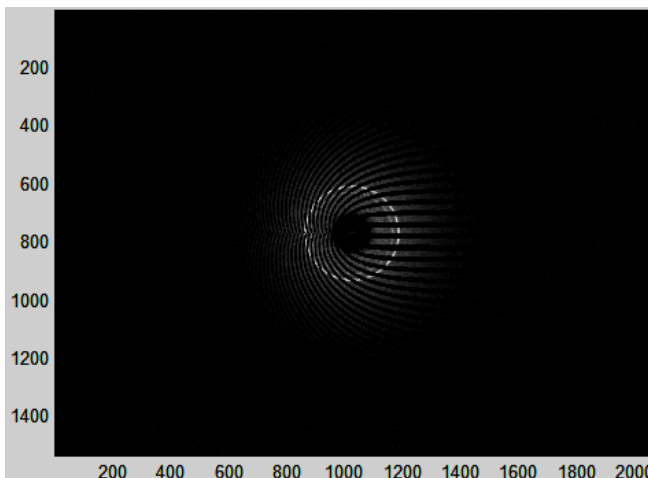
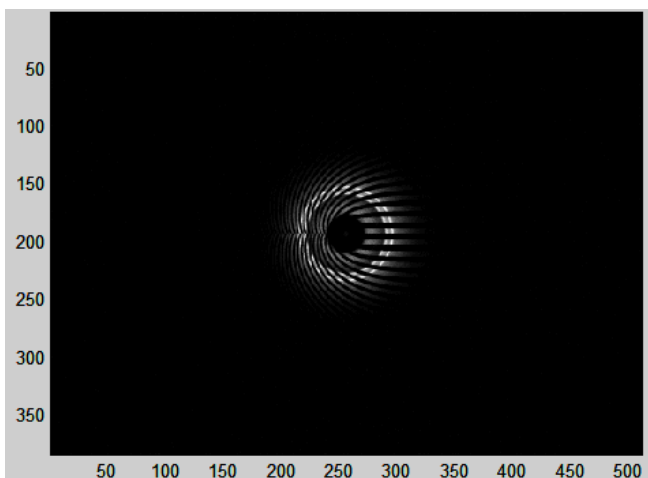
- Underlying characteristic of a target of interest under X-ray illumination
 - Employed to identify specific targets
 - Coherent scatter, incoherent scatter, attenuation
- Defined in three different spaces
 - Measured (Detector or measurement space)
 - Reconstructed (Target or object space)
 - Compressed (Logical or abstract space)
- Measured and reconstructed are acquired via experiments and/or MC simulations
- Compressed acquired via system design and integration



Example Signatures – Measurement Space (pencil beam, target alone)



Acrylic



Graphite

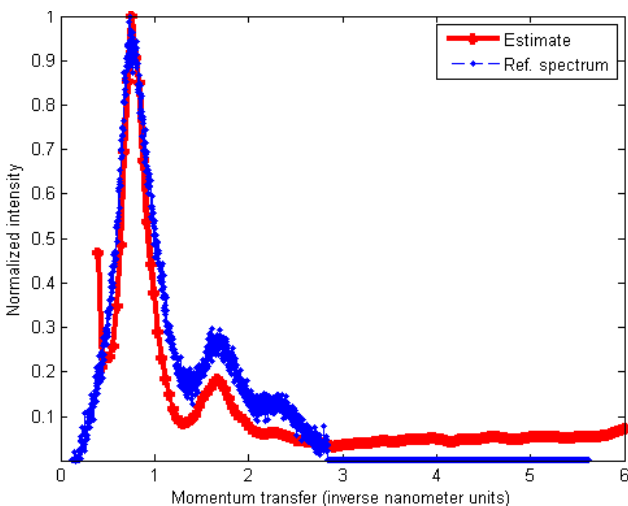
150kVp, 0.1mm W

150kVp, No Filter

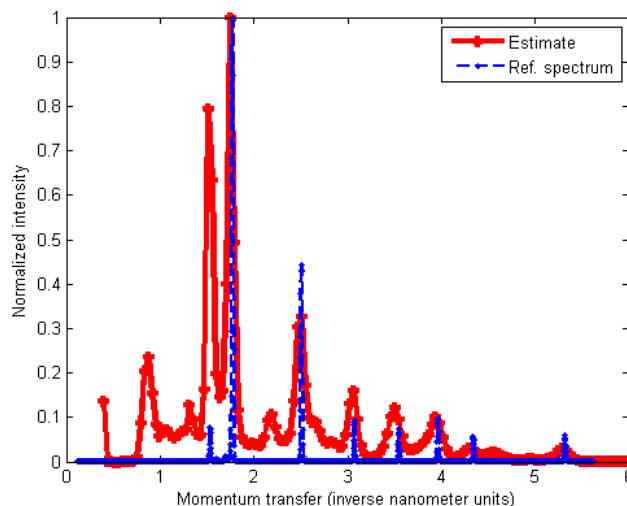


Example Signatures – Target Space (150kVp, 0.1mm W)

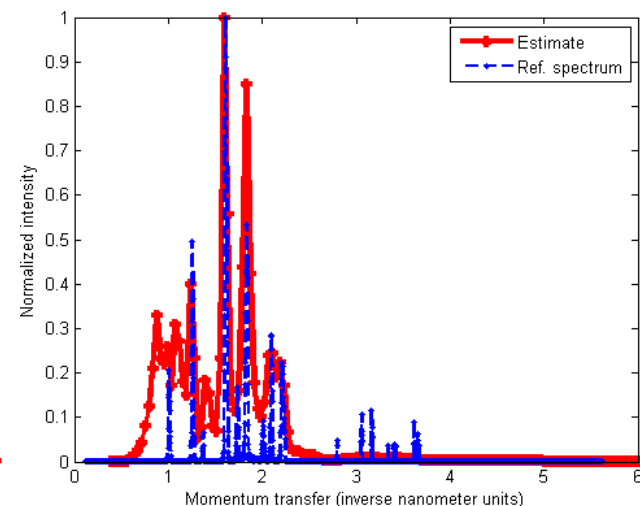
Acrylic



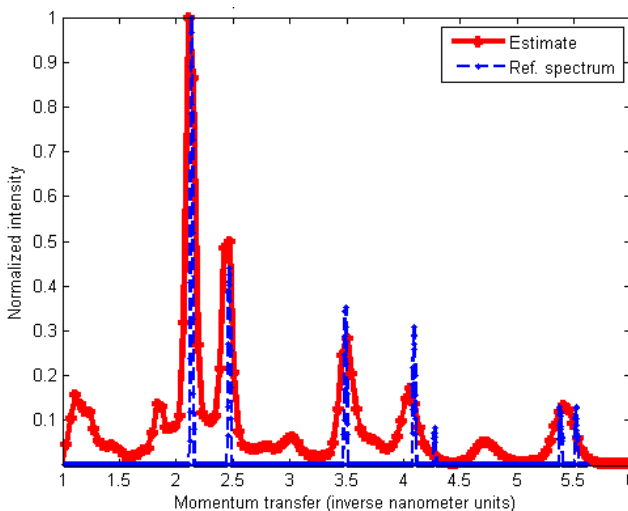
NaCl



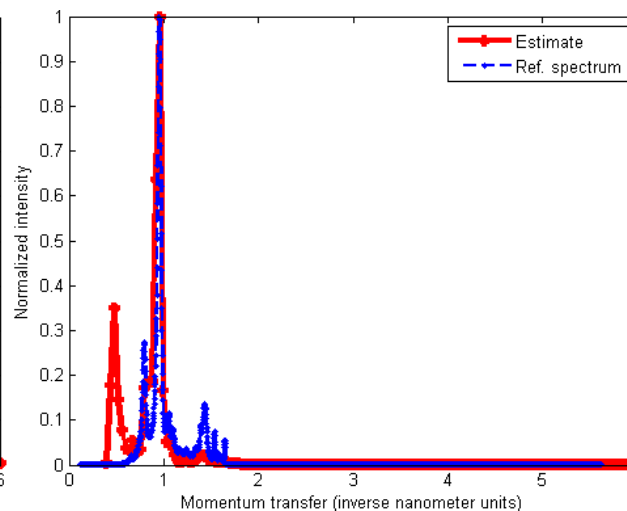
NH₄NO₃



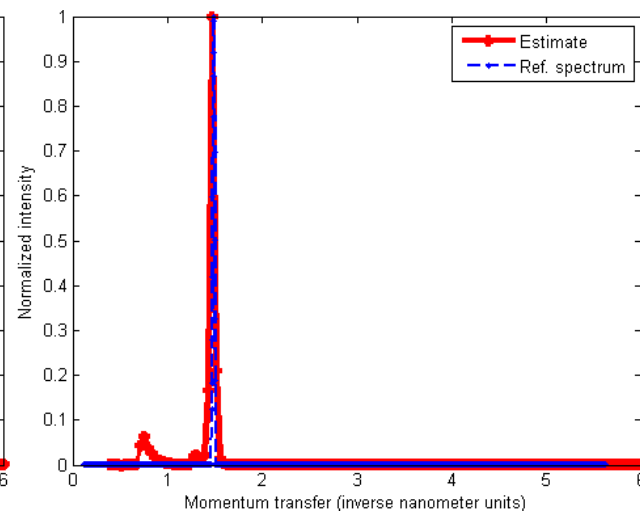
Al



Milk chocolate

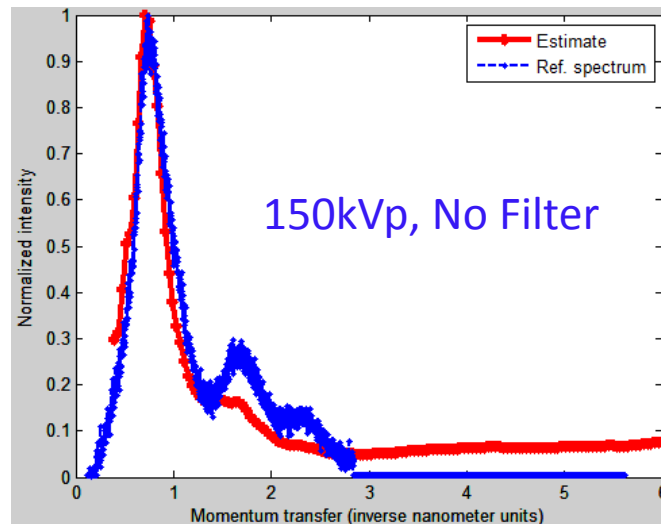
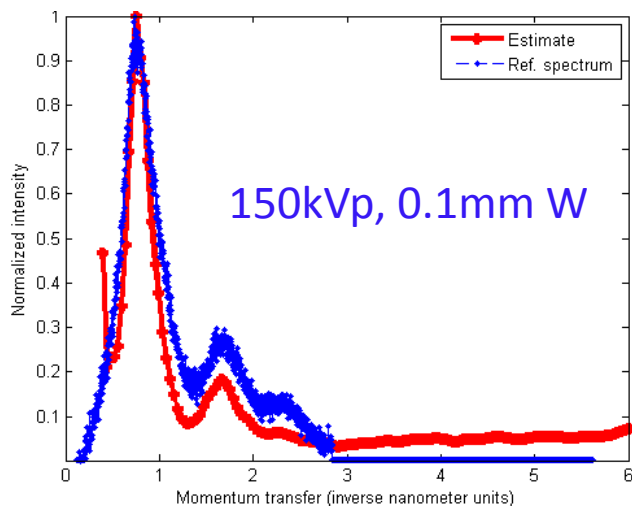


Graphite

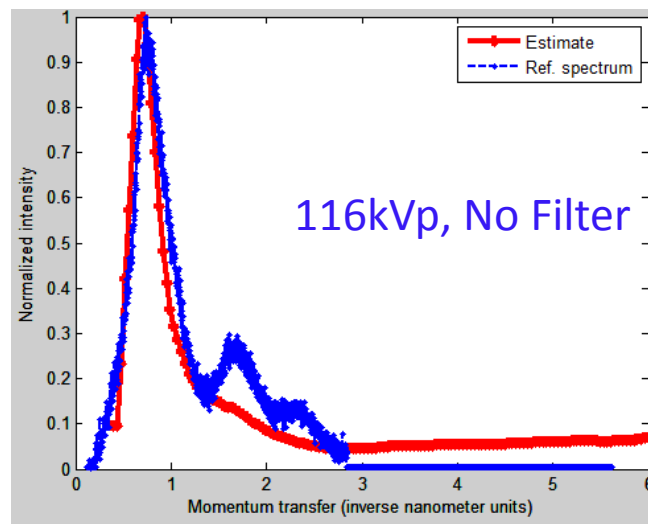
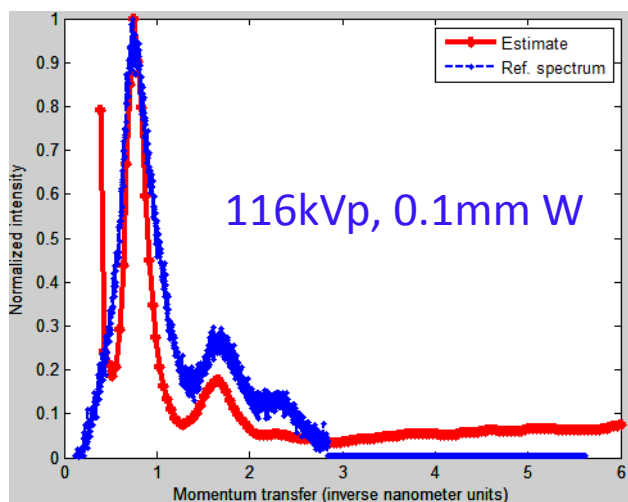




Reconstructed signature with different spectra

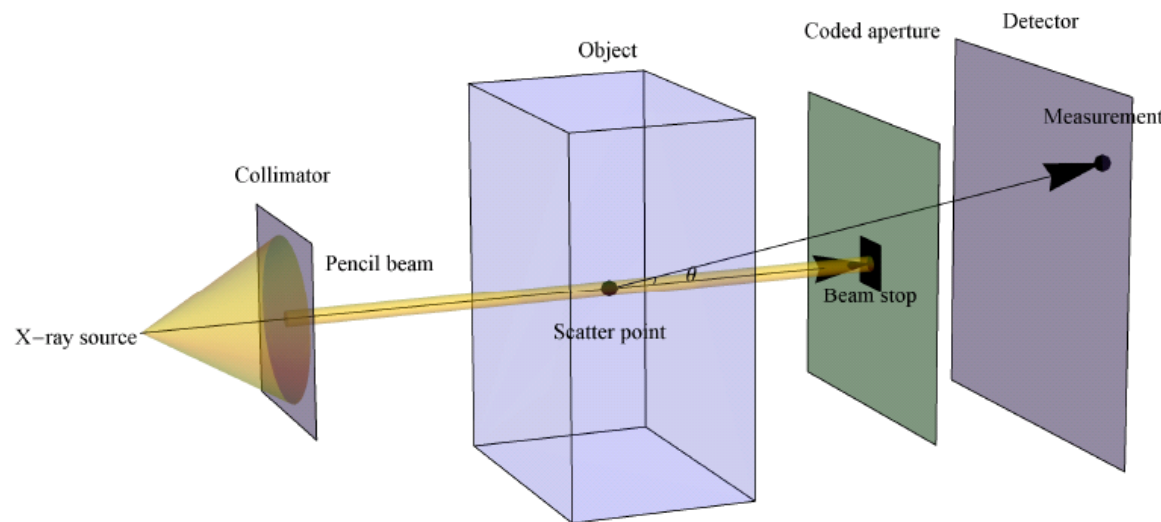


Acrylic

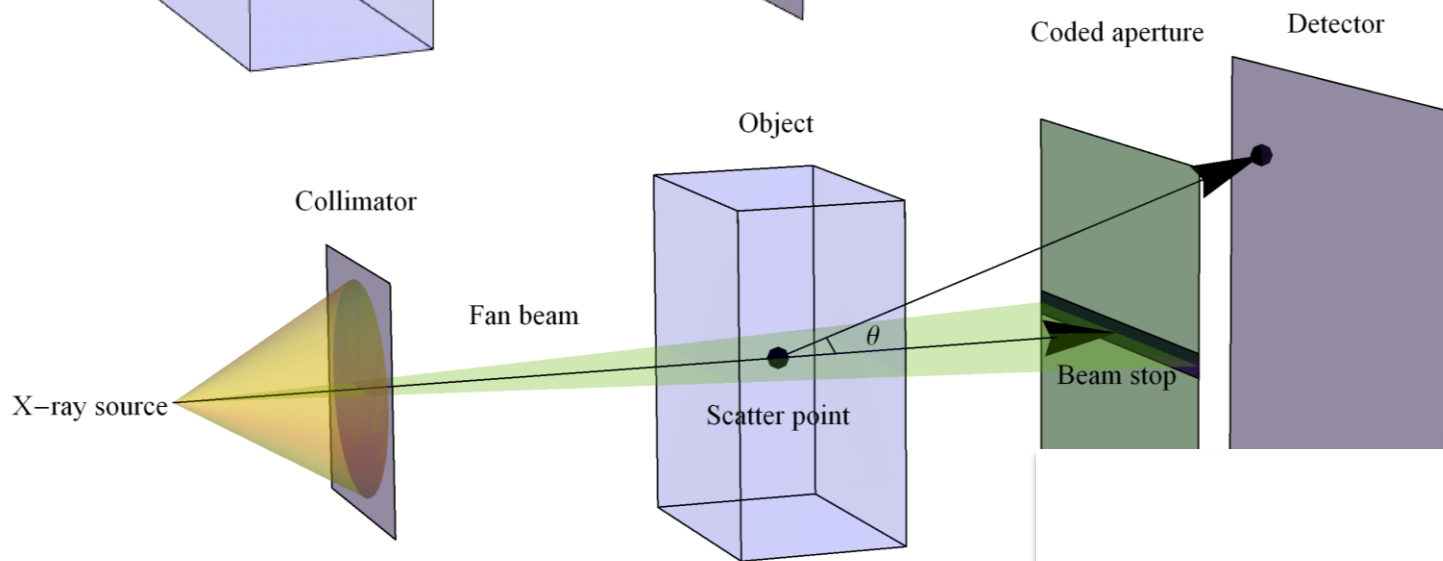




Pencil Beam \rightarrow Fanbeam Model



$\mathbf{r} = [x, y, 0]$,	object point
$\mathbf{r}' = [X_d, y', z']$,	detector point
θ ,	scatter angle
$\mathbf{s} = \mathbf{r}' - \mathbf{r}$,	scatter vector





Physics-Based Model

- Based on a radiance model, propagated using ray projection
- Objects have scattering densities f at each spatial location \mathbf{r} , as a function of momentum transfer q
- For coherent scatter at angle θ , Bragg's Law gives $q=2k\sin(\theta/2)$
- Given vector \mathbf{s} from scattering point to detector whose normal is \mathbf{n} , there is a geometric factor $\frac{|\mathbf{n} \cdot \hat{\mathbf{s}}|}{s^2}$, where $\mathbf{s} = \mathbf{r}' - \mathbf{r}$
- Mask factor $T(\mathbf{r}, \hat{\mathbf{s}})$
- Detector response $g(\mathbf{r}')$ in terms of impulse response

$$g(\mathbf{r}') = \int dA \int dq H(\mathbf{r}', \mathbf{r}, q) f(\mathbf{r}, q)$$

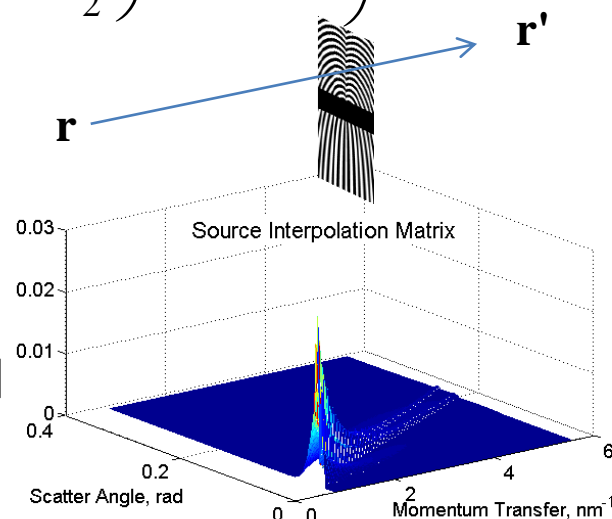
$$H(\mathbf{r}', \mathbf{r}, q) = \frac{C}{dA} \left| \frac{\mathbf{n} \cdot \hat{\mathbf{s}}}{s^2} \right| T(\mathbf{r}, \hat{\mathbf{s}}) \left(\frac{1}{2q \sin \frac{\theta}{2}} \right) W \left(\frac{q}{2 \sin \frac{\theta}{2}} \right)$$



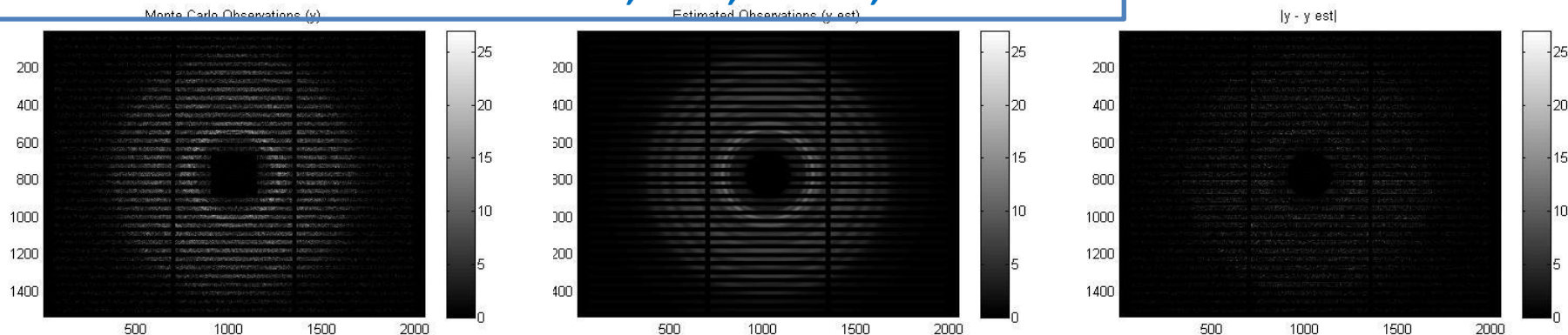
Computation: Forward Model

$$g(\mathbf{r}') = C \int d\mathbf{r} \left(\left| \frac{\mathbf{n} \cdot \hat{\mathbf{s}}}{s^2} \right| T(\mathbf{r}, \hat{\mathbf{s}}) \int dq \left(\frac{1}{2q \sin \frac{\theta}{2}} \right) W \left(\frac{q}{2 \sin \frac{\theta}{2}} \right) f(\mathbf{r}, q) \right)$$

- Detector response = Integrate object points \times geometry factor \times mask \times integrate object momenta at scatter angle
- There exist opportunities to exploit symmetry
- Efficient computations have been implemented
- Backward model is the adjoint operator



Monte Carlo Pencil Beam Data of Al; Data, Model , Residual





Log-likelihood for Poisson Data

$$g(\mathbf{r}') = \int dA \int dq H(\mathbf{r}', \mathbf{r}, q) f(\mathbf{r}, q) \rightarrow \mathbf{g} = \mathbf{H}\mathbf{f}$$

$$g(m) = \sum_{i \in I} h(m, i) f(i)$$

- Forward model predicts the mean detector values
- A Poisson model is appropriate in many applications. Denote the random data by

$$y(m) \square \text{Poisson} \left(\sum_{i \in I} h(m, i) f(i) + \mu_b(m) \right), \quad m \in M$$

- The log-likelihood function for the data is

$$l(\mathbf{y} | \mathbf{f}) = \sum_{m \in M} y(m) \ln \left(\sum_{i \in I} h(m, i) f(i) + \mu_b(m) \right) - \left(\sum_{i \in I} h(m, i) f(i) + \mu_b(m) \right)$$

where $\mu_b(m)$ is the mean number of background counts

- Penalized ML estimation (also MAP); alternatively, variational Bayes (L. Carin, et al.)

$$\hat{\mathbf{f}}_{PML} = \arg \max_{\mathbf{f}} l(\mathbf{y} | \mathbf{f}) - \beta \varphi(\mathbf{f})$$

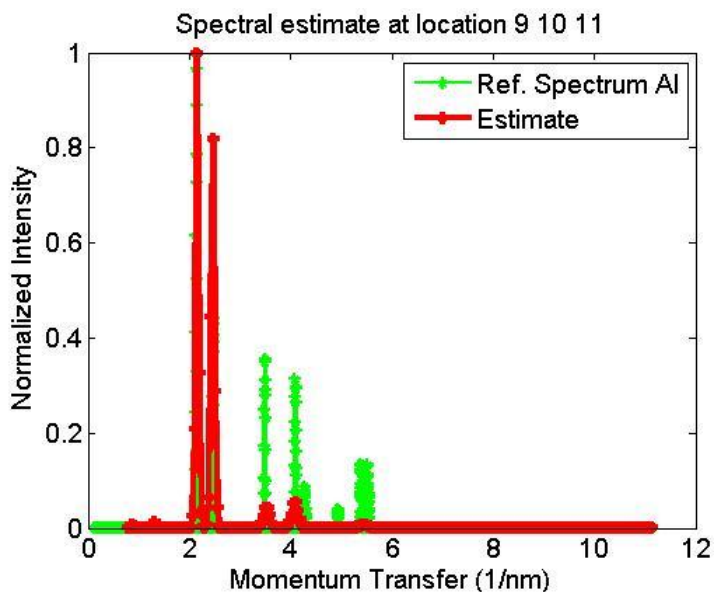


Pencil Beam Data, Forward Model and Monte Carlo

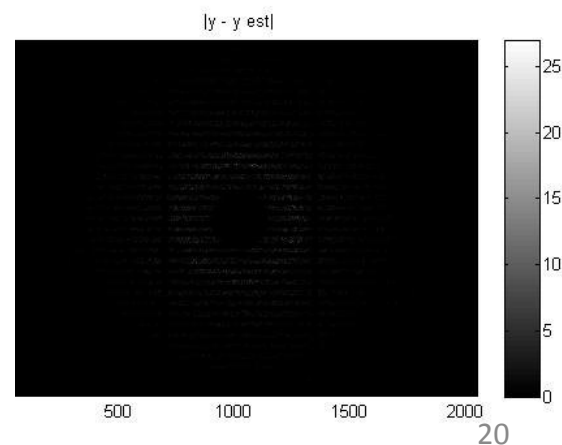
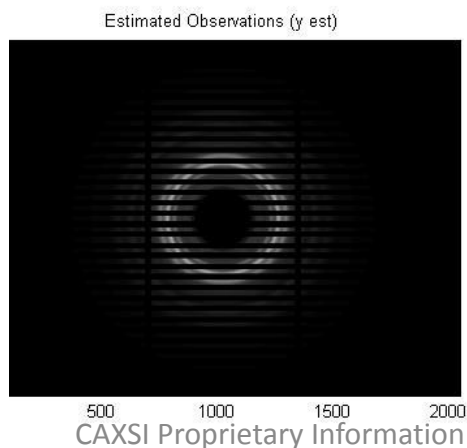
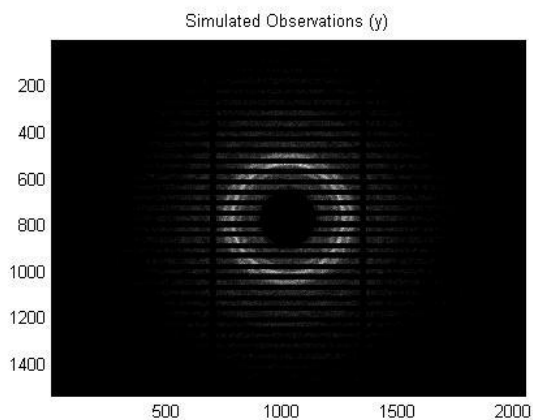
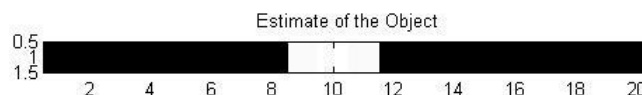
- Simulation parameters:
 - source to mask distance = 94.77 cm,
 - source to object distance = 57.78 cm,
 - source to detector distance = 109.47 cm.
- During reconstruction,
 - x resolution = 0.4 cm,
 - Number of pixels = 20,
 - momenta = 10:0.5:140,
 - downsampling factor = 1
- Simulated data: Al points at $x = 9, 10, 11$
- Monte Carlo data



Pencil Beam Data, Forward Model After 5 Iterations

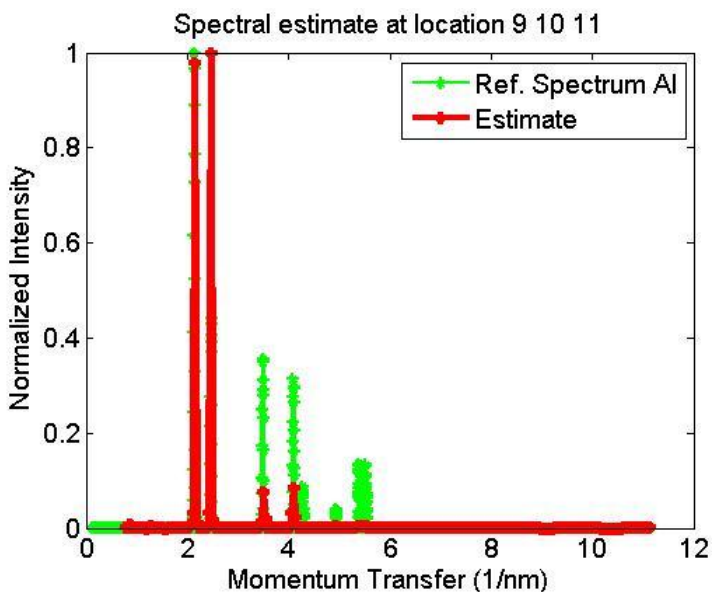


- The true Al spectrum, and the spectral estimate at location 9, 10, 11.
- Ave. of the reconstructed object over the momentum transfer coordinate.
- Simulated detector data with Poisson noise (Maximum detector value set at 50).
- Estimated detector data.
- Absolute difference between the noisy simulated and estimated data.

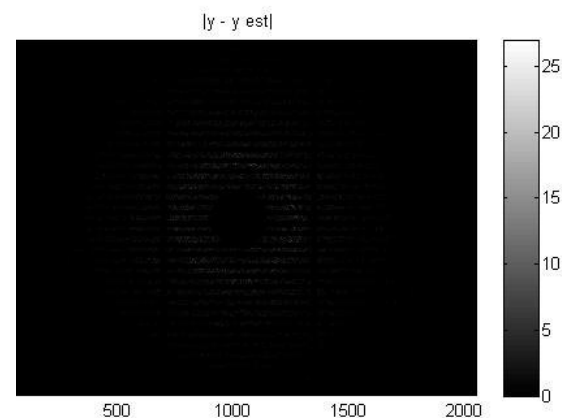
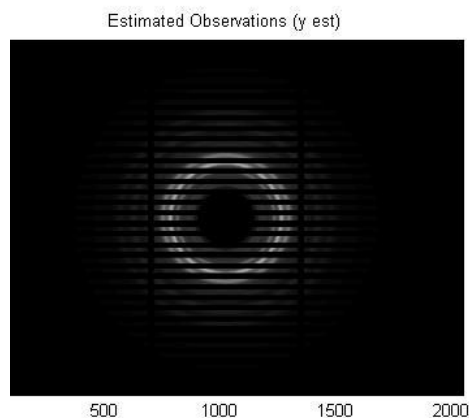
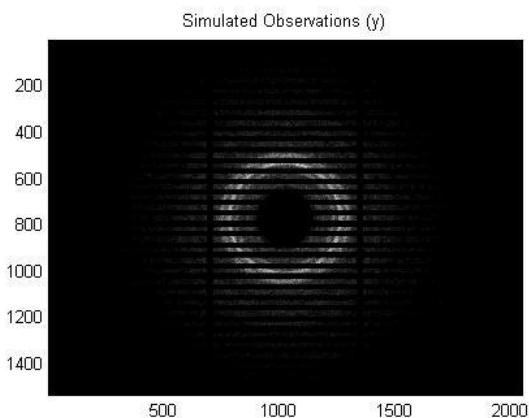
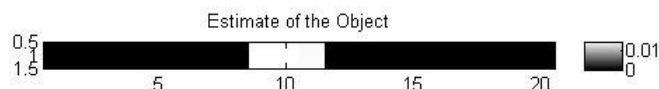




Pencil Beam Data, Forward Model After 200 Iterations

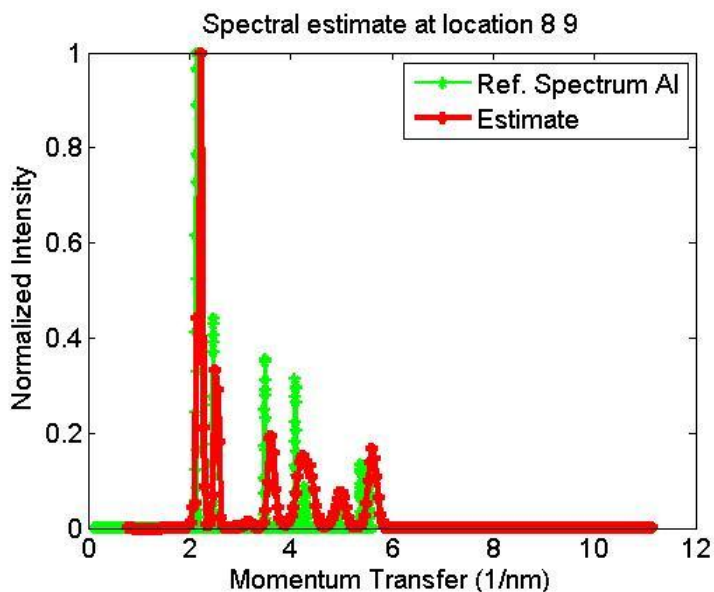


- The true Al spectrum, and the spectral estimate at location 9, 10, 11.
- Ave. of the reconstructed object over the momentum transfer coordinate.
- Simulated detector data with Poisson noise (Maximum detector value set at 50).
- Estimated detector data.
- Absolute difference between the noisy simulated and estimated data.

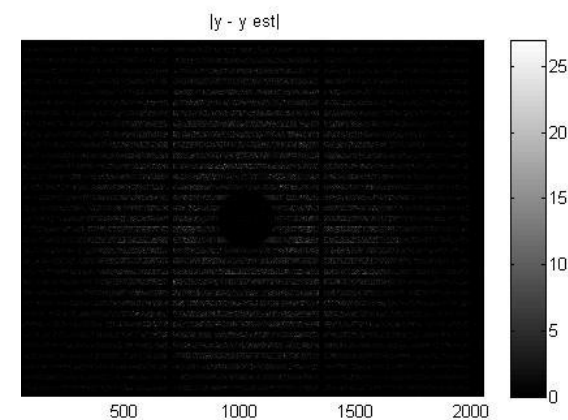
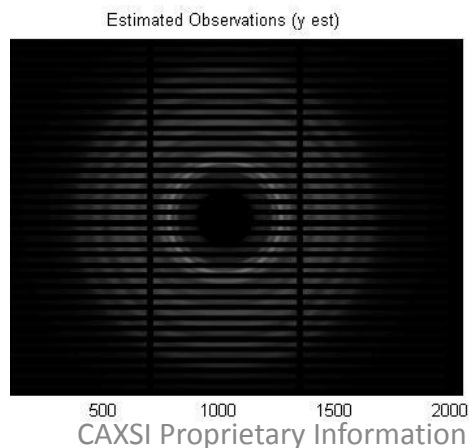
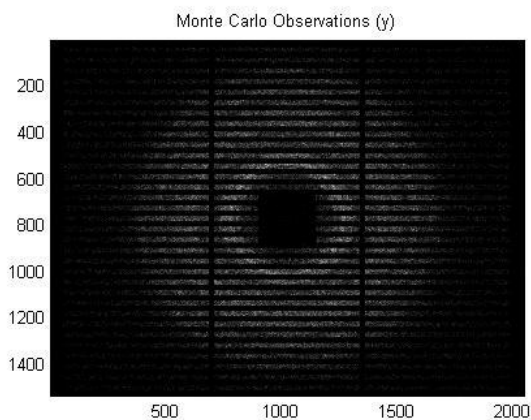
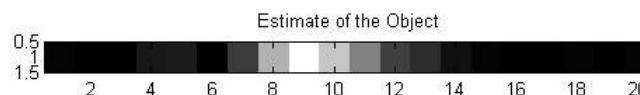




Pencil Beam Data, Monte Carlo After 5 Iterations

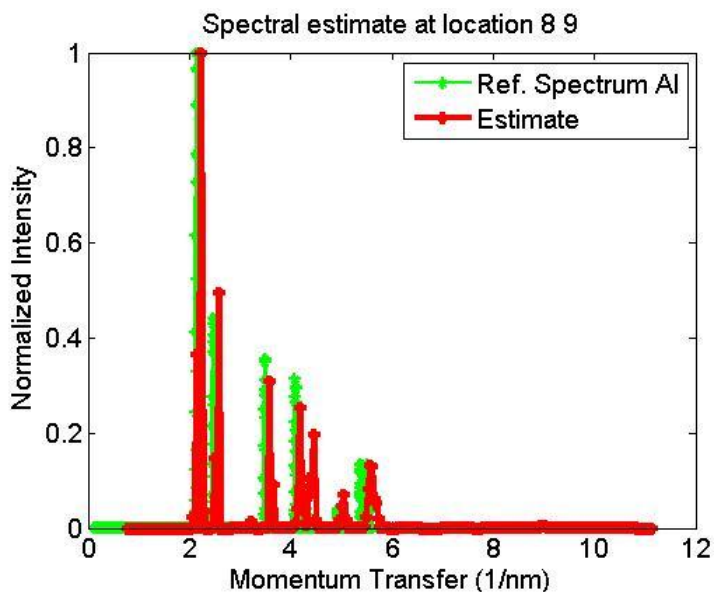


- The true Al spectrum, and the spectral estimate at location 8, 9.
- Ave. of the reconstructed object over the momentum transfer coordinate.
- The noisy Monte Carlo pencil beam data.
- Estimated detector data.
- Absolute difference between the noisy Monte Carlo and estimated data.

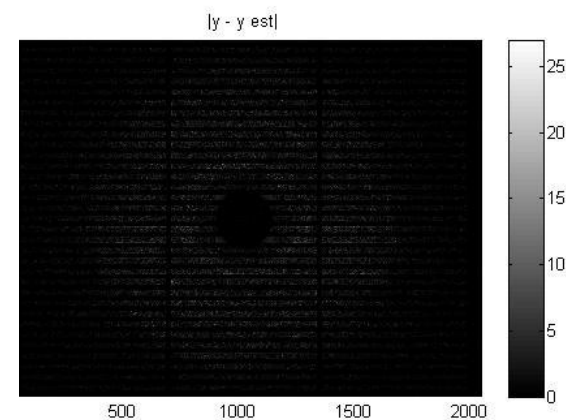
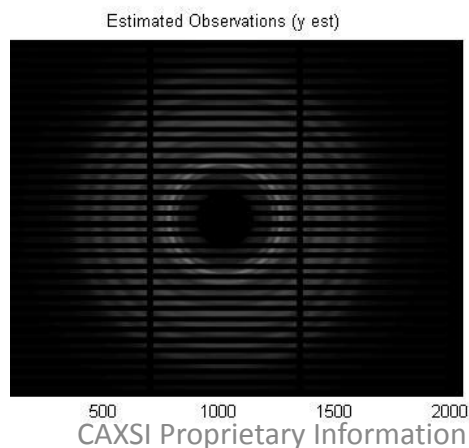
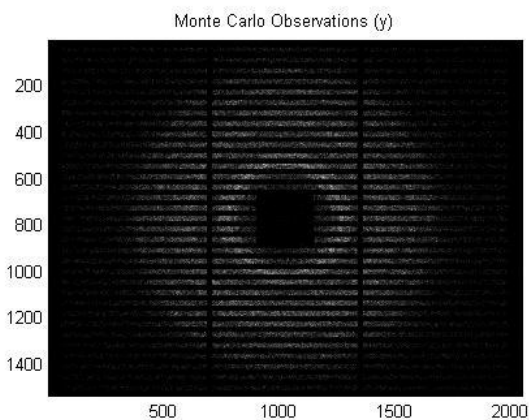
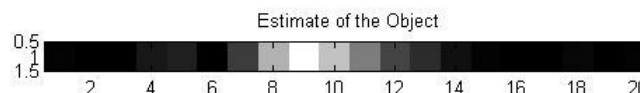




Pencil Beam Data, Monte Carlo After 200 Iterations

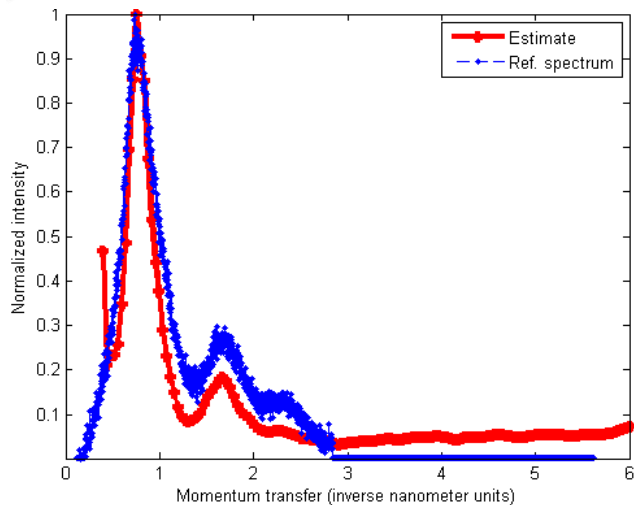


- The true AI spectrum, and the spectral estimate at location 8, 9.
- Ave. of the reconstructed object over the momentum transfer coordinate.
- The noisy Monte Carlo pencil beam data.
- Estimated detector data.
- Absolute difference between the noisy Monte Carlo and estimated data.

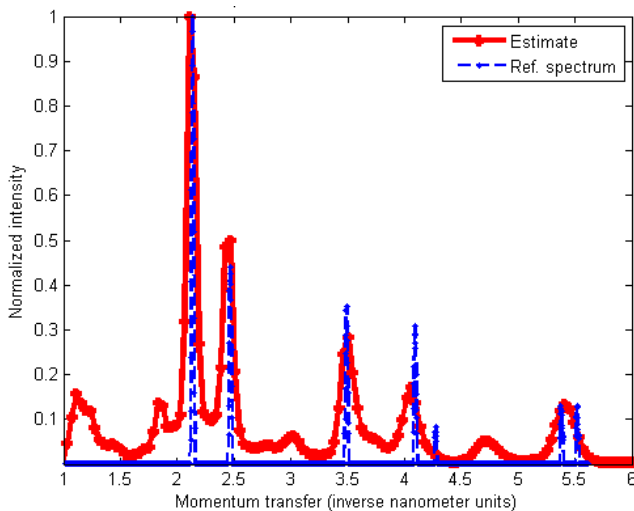




Target Signatures: Amorphous vs. Crystalline



Acrylic



Aluminum

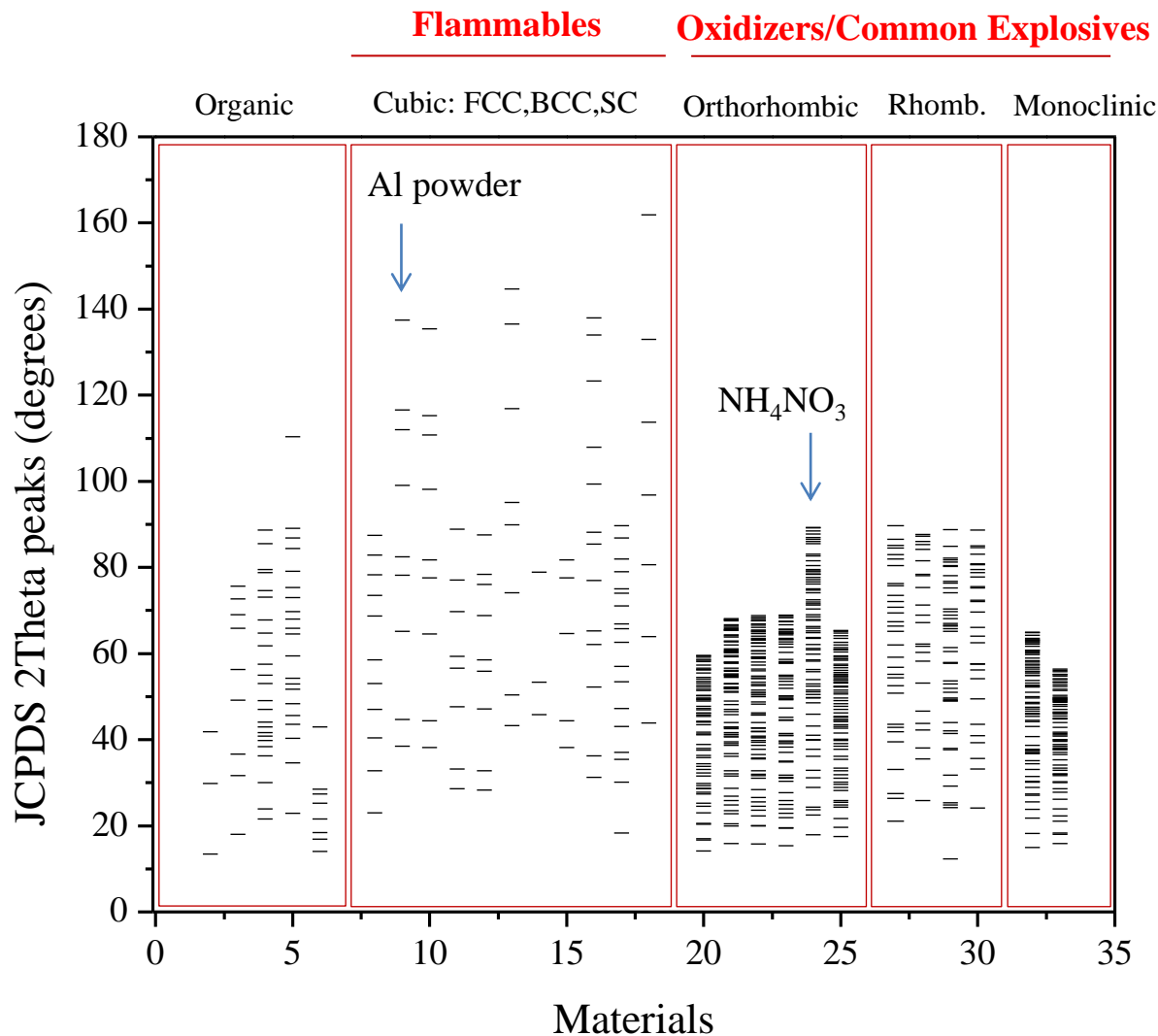
Crystal system: Cubic

Crystal lattice: Face-centered
(Face-centered cubic, FCC)

Diffraction spectra are dependent on crystal structure



Classification based on materials crystallinity

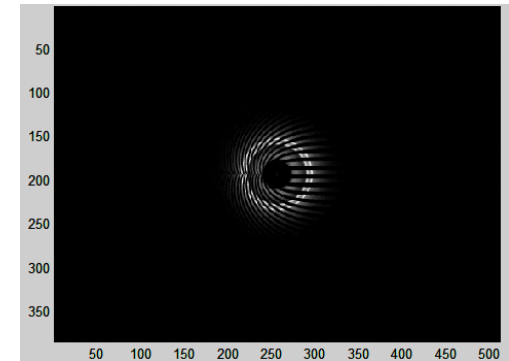
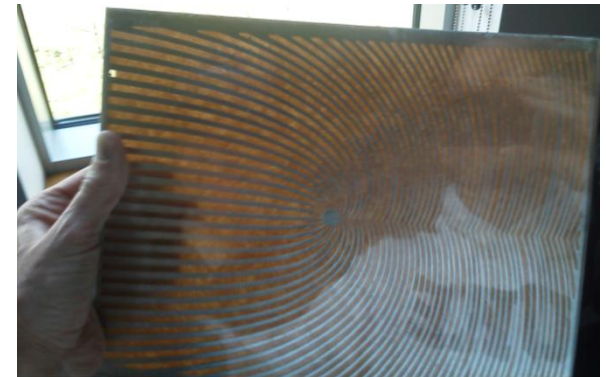
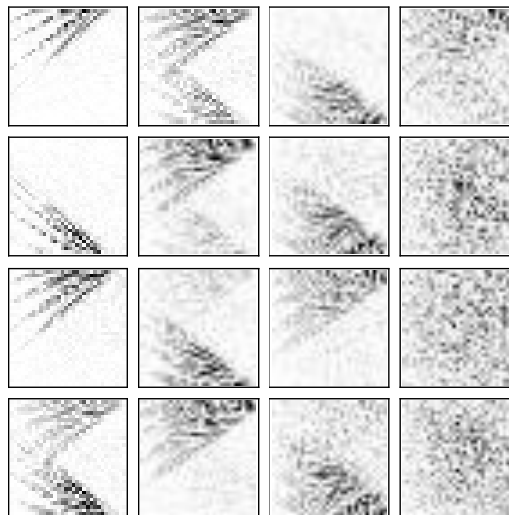


Indexing texture of diffraction pattern may aid in fine-tuning material classification

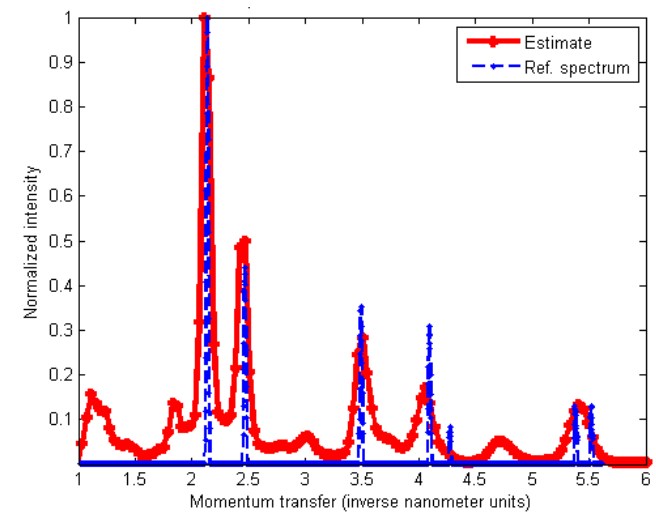


CAXSI Outline

- CAXSI System Vision
- Signature Analysis
 - Measurement space signature
Forward models
 - Object space signature
Reconstruction
 - Logical space signature
SVD
- Conclusion

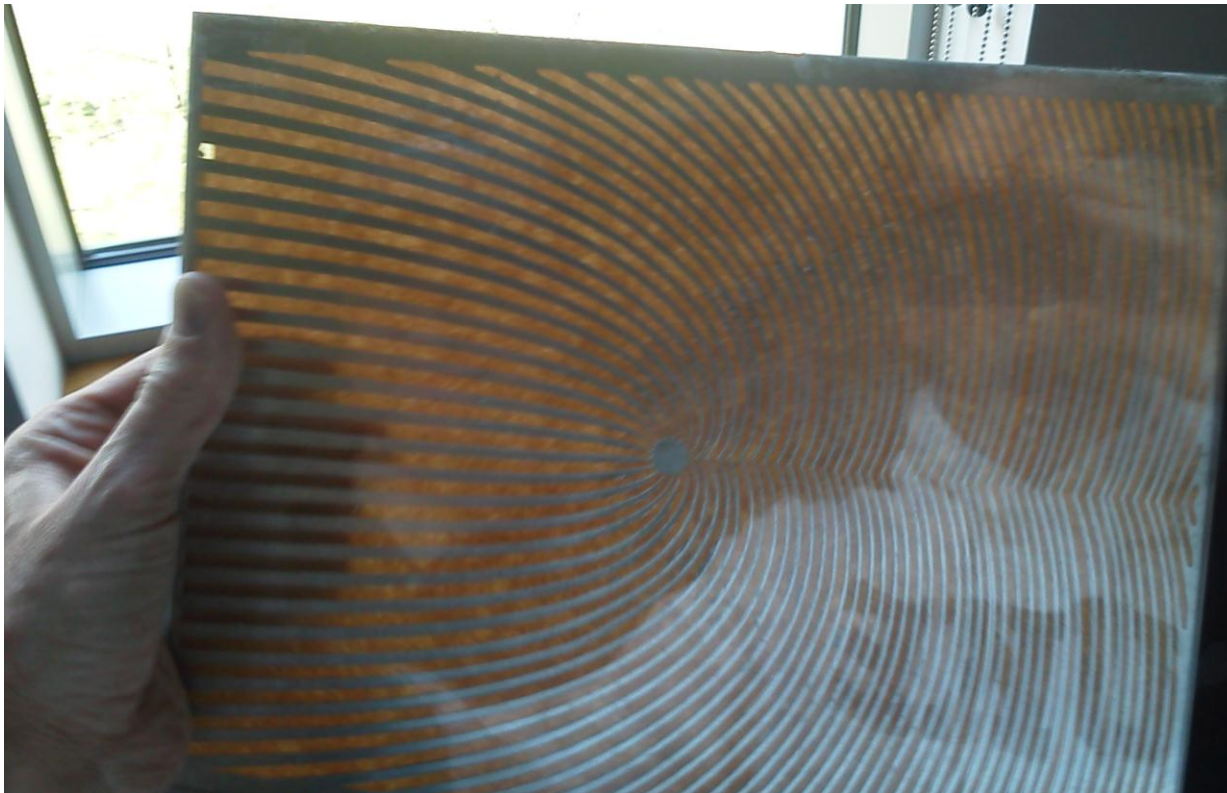


AI



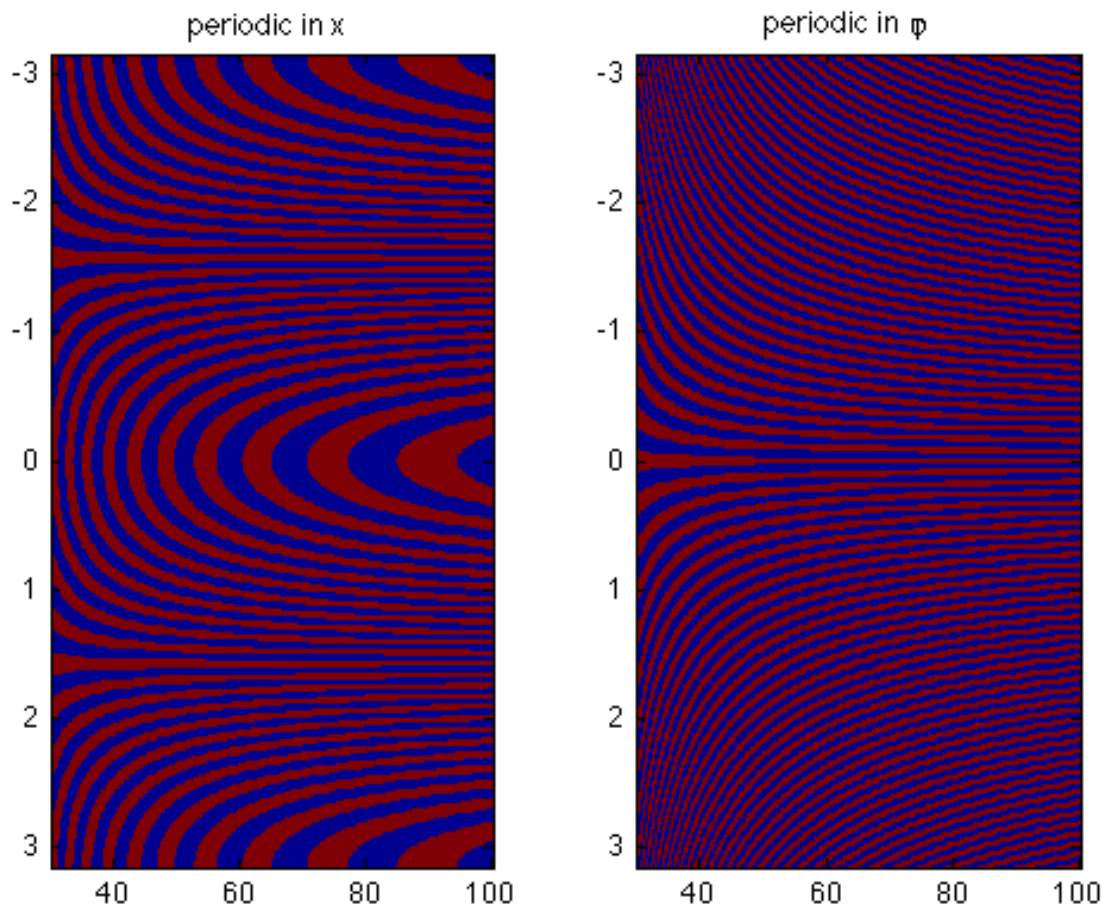


Design for Sampling Structure and Conditioning





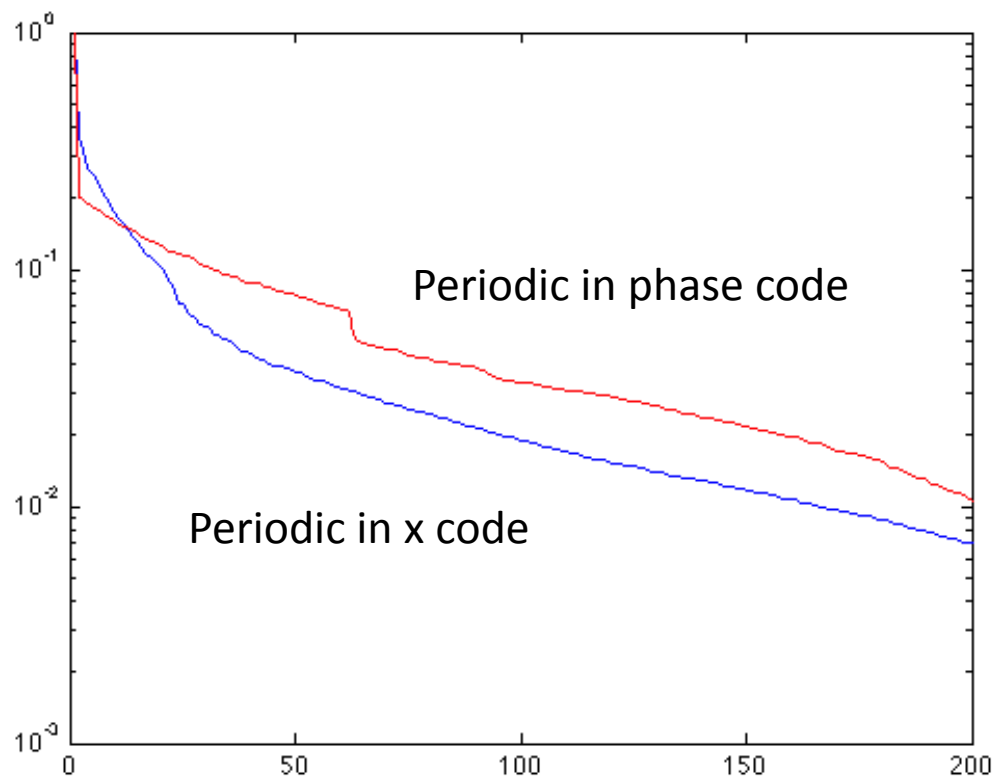
Visibility in radius and angle





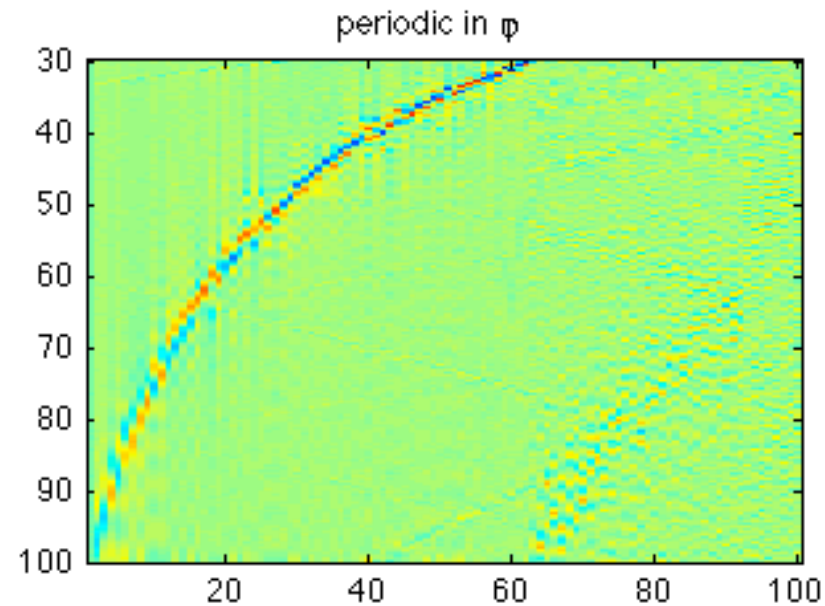
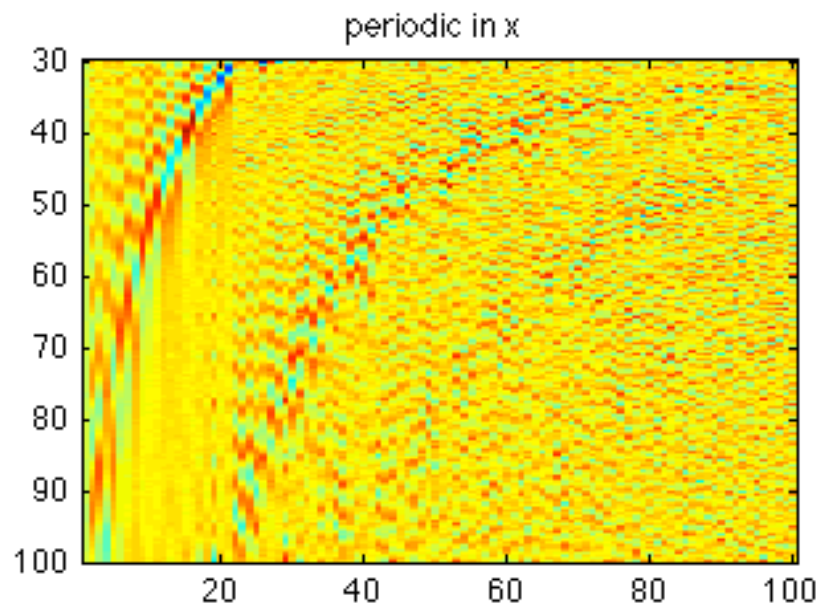
Singular Values

Pencil Beam, Coded Aperture





Singular Vectors





Singular value analysis of coded aperture x-ray scatter imaging

David J. Brady* and Daniel L. Marks

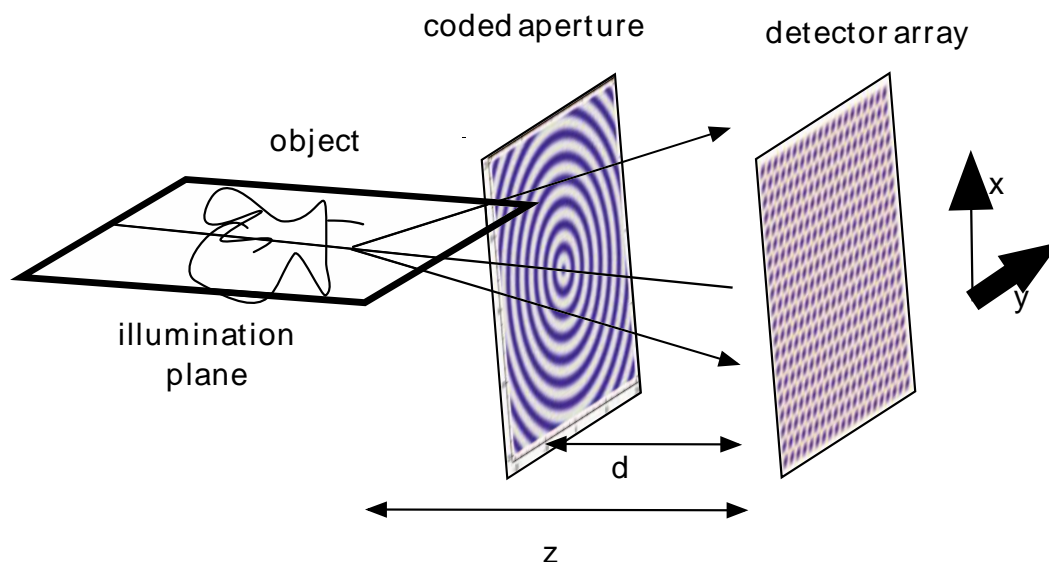
Fitzpatrick Institute for Photonics and Department of Electrical and Computer Engineering
Duke University, P.O. Box 90291, Durham NC 27708

* Corresponding author: dbrady@duke.edu

Compiled July 4, 2012

We examine the conditioning and singular value spectra of tomographic coded aperture scatter imagers. Scatter imaging may enable tomography of compact regions from snapshot measurements with singular values scaling favorably as compared to the Radon transform. The scaling of the singular value spectrum of the 2-D fan-beam geometry is confirmed through simulations. © 2012 Optical Society of America

OCIS codes: 110.6955, 110.7440.



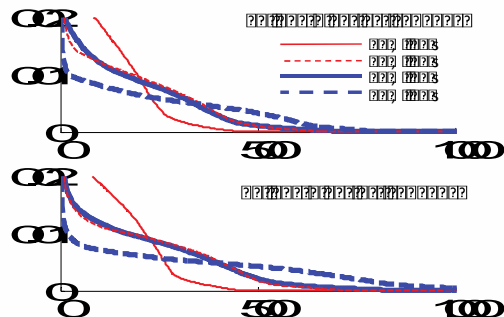
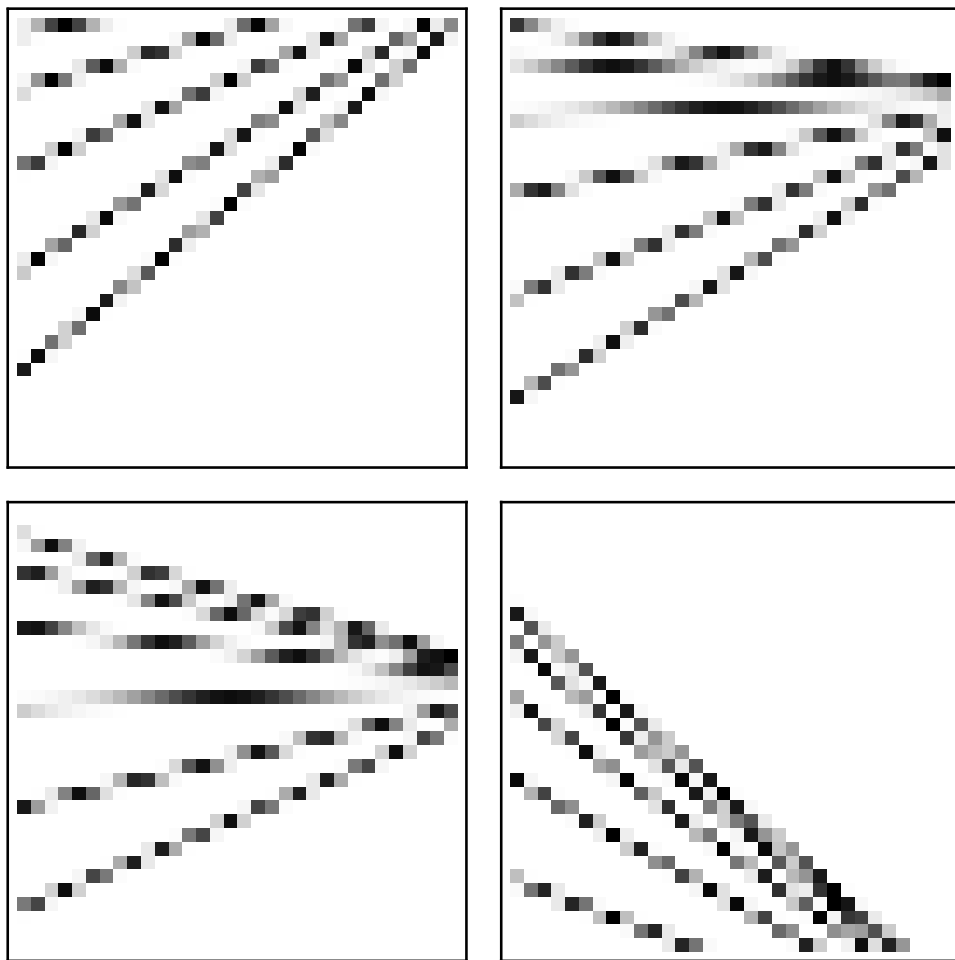


Fig. 3. Singular value spectra for (a) $L = 23$ length quadratic residue code and $L = 47$ length quadratic residue code. The four curves indicate differing number of samples measured in the H (shift code) direction, and the V (scale code) direction.

Illumination	CAXSI	Selected Volume	Radon
Pencil	$\frac{\sqrt{\Omega}}{N}$	$\frac{1}{N}$	$\frac{1}{N}$
Plane	$\frac{\sqrt{\Omega}}{N^2}$	$\frac{1}{N^2}$	$\frac{1}{N}$
Volume	$\frac{\sqrt{\Omega}}{N^3}$	$\frac{1}{N^3}$	$\frac{1}{N}$



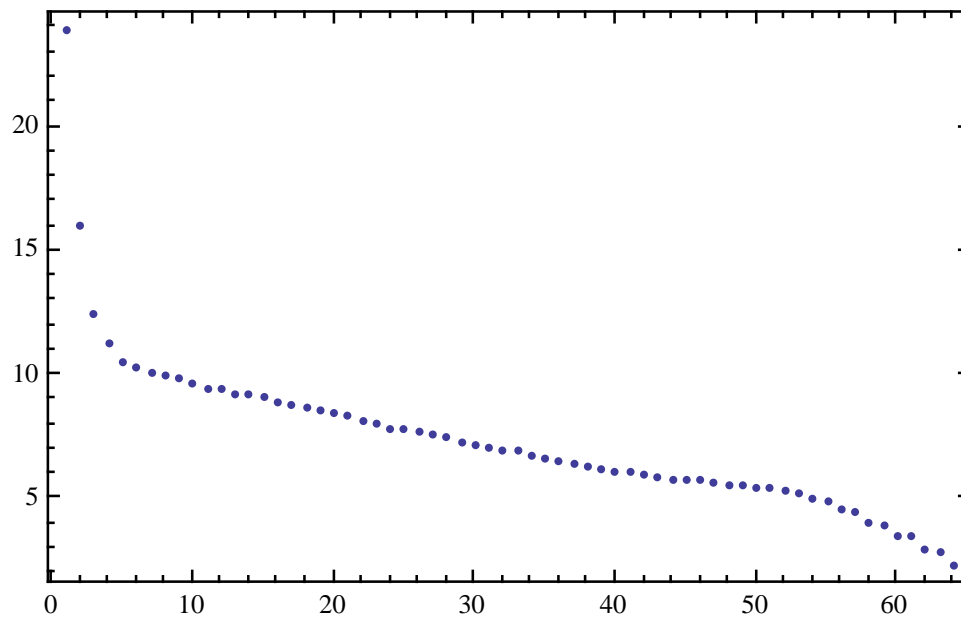
Multiple Source Illumination



Sensor sensitivity

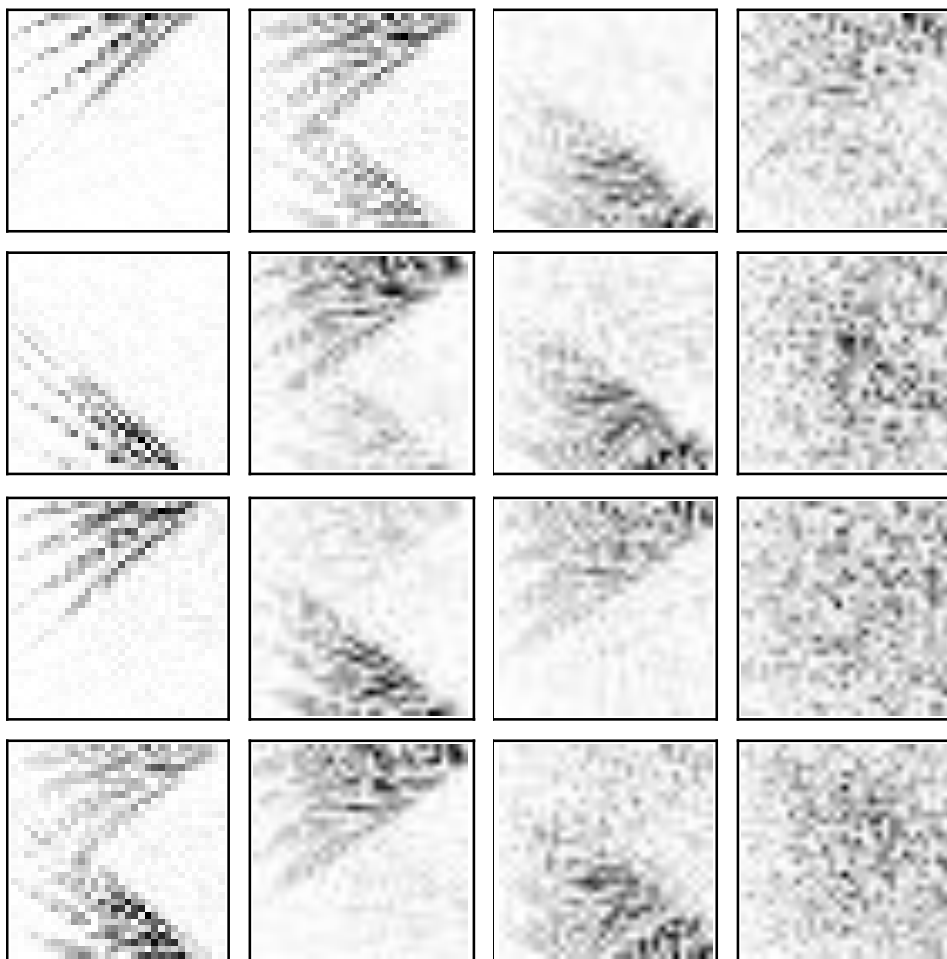


Singular Values



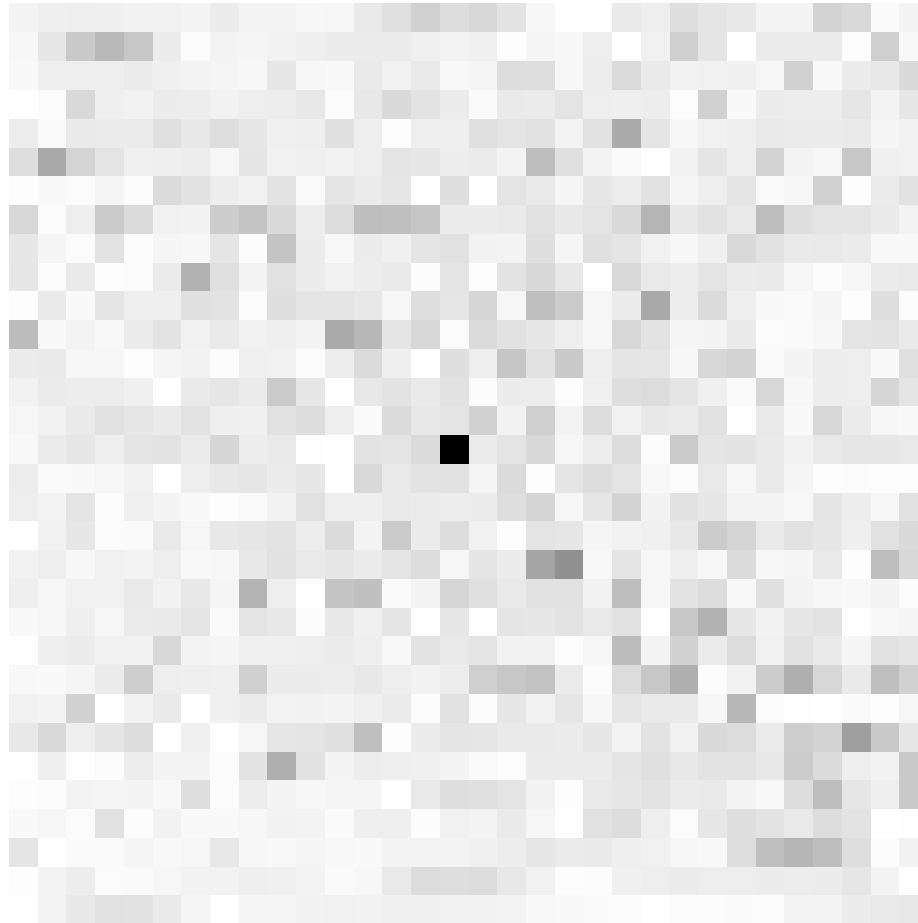


Singular Vectors



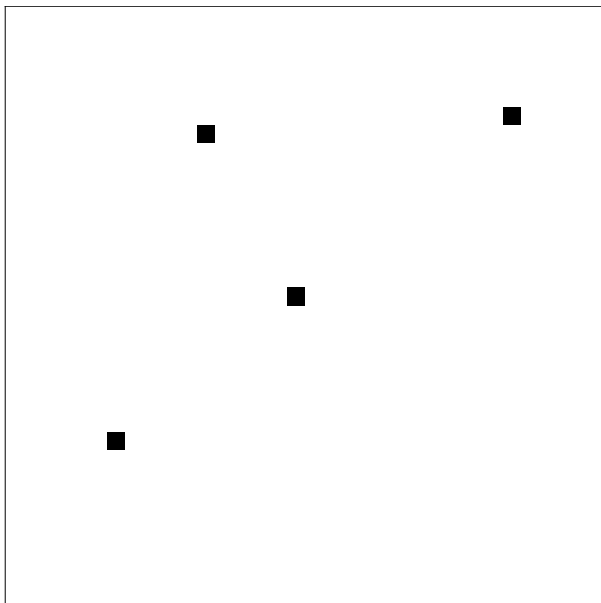


Point Target Reconstruction





Multiple Points





SVD and Design

- Linear response functions map generalized measurement and include detector response, source structure, object basis (dictionaries)
- Restricted isometry, source similarity etc. can be analyzed
- Linear response guides design, feeds classification engines
- System response feeds adaptive structure



Example Specifications: Knowledge-Enhance Compressive Measurements

Tunnel geometry	60 by 40 cm 10 by 10 cm?
Source(s)	1-4 sources, multifan collimation
Beam Energy	150-160 KV
Image resolution	1.5 mm cube
Momentum resolution	0.1 nm^{-1}
System volume	3.3 (L) by 1.3 (W) by 1.3 (H) meters
Pixel size	1 mm
Number of pixels	750 for attenuation signals 5,000 scatter pixels, including 128 energy resolving pixel.



KECoM AT

